PHYSICAL REVIEW D VOLUME 22, NUMBER 7 1 OCTOBER 1980

Quark-parton model of nuclear production

G. Berlad, A. Dar, and G. Eilam
Department of Physics, Technion-Israel Institute of Technology, Haifa, Israel
(Received 22 January 1980)

We propose a quark-parton model of a nucleus viewed in a high-momentum frame. We use it to calculate deep-inelastic lepton scattering, lepton pair production, W-boson production, particle production at large x and small p_T, and cumulative production of particles at backward angles in high-energy hadron-nucleus collisions. Predictions are compared with experimental data. Good agreement between theory and experiment is demonstrated.

I. INTRODUCTION

The past few years have witnessed a fast increase of interest in studying high-energy particle-nucleus collisions.[1] This is partly due to practical advantages (larger cross sections, better mechanical properties, and a better heat conductivity) of nuclear targets compared with proton targets, partly due to theoretical advantages (e.g., possibilities to test theoretical models over a wider range of target quantum numbers, to study nonasymptotic states via rescattering inside the nucleus, and to filter out specific processes), and partly due to observations of unexpected dependence of cross sections on the atomic number A of the target nucleus[1] (e.g., cumulative production and anomalous A dependence). However, while considerable progress has been made during the past few years in understanding hadrons in terms of the quark-parton model[2] and its possible underlying field theory, quantum chromodynamics[3] (QCD), very little progress has been made toward a quantitative understanding of high-energy particle-nucleus interactions in terms of the quark-parton model and QCD. In the present paper and in a forthcoming publication we shall show that a quark-parton model of the nucleus and QCD can correctly predict nuclear cross sections and their surprising A dependence. In fact the agreement which is obtained between theory and experiment is remarkable.

The quark-parton model of hadrons[2] views an energetic hadron (i.e., a hadron in an "infinite-momentum frame") as composed of valence quarks (which carry its quantum numbers) and of a neutral sea of gluons and quark-antiquark pairs. The quarks and gluons are pointlike constituents which behave as free when they absorb a quantum with large energy and momentum. A justification for the quark-parton model is provided by QCD: In QCD quarks (of three colors) interact with eight colored gluons (massless vector bosons) and this interaction binds and confines the quarks to give color singlet hadrons. Being asymptotically free, QCD provides a leading behavior in processes where large momentum transfers are involved. It gives Bjorken scaling[4] (modulo logarithmic corrections) in deep-inelastic lepton-hadron scattering and the behavior of cross sections for inclusive production of hadrons with large transverse momentum ($p_T \gtrsim 1$ GeV/c). However, processes which involve large momentum transfers have very small cross sections and hadron production is completely dominated by production of hadrons with small p_T. Such soft processes in QCD require a nonperturbative approach which is still lacking and it has not been possible so far to use it to explain the bulk of the experimental data on hadron-hadron collisions. Nevertheless, attempts to understand some soft processes in hadron-hadron collisions in terms of quarks and gluons[5] have enjoyed a qualitative success. In this paper we shall show that the general picture underlying this qualitative success of the quark-parton model for some soft processes is sufficient to obtain a successful quantitative description of their A dependence.

Our paper is organized as follows: In Sec. II we present our quark-parton picture of a nucleus in a high-momentum frame, from which we derive quark distributions in ultrarelativistic nuclei. Various production cross sections from nuclear targets are then calculated and compared with experimental data. In Sec. III we discuss briefly deep-inelastic lepton scattering from nuclei, in Sec. IV lepton pair production in hadron-nucleus collisions, in Sec. V W-boson production, in Sec. VI particle production with small p_T and large x, and in Sec. VII cumulative particle production at backward laboratory angles are discussed. Finally in Sec. VIII we draw some general conclusions.

II. THE QUARK-PARTON STRUCTURE OF A FAST NUCLEUS

Current models of particle production from hadron targets at high energies require a knowledge

 © 1980 The American Physical Society

of the momentum distribution of the quarks and gluons in the target when it is viewed from a high-momentum frame. To extend these models to particle production from nuclear targets one needs to know the momentum distributions of quarks and gluons in ultrarelativistic nuclei. These distributions can either be extracted from deep-inelastic leptoproduction from nuclear targets or be estimated from theoretical models.

In QCD colored quarks interact strongly via exchange of colored gluons. These interactions are believed to bind and confine three colored quarks to give color singlet nucleons. Being color singlets the nucleons cannot interact strongly via an exchange of a single colored gluon. Thus binding forces between nucleons in nuclei are small compared with binding forces within nucleons. (The average binding energy per nucleon in a nucleus is about 8 MeV while the nucleon rest mass is about 1 GeV.) Therefore it is useful to consider a nucleus in its rest frame as a bound state of point-like nucleons. However, when a nucleus moves with a relativistic velocity its nucleons look as if they are composed of valence quarks and of a neutral sea of gluons and quark-antiquark pairs. Thus the momentum distribution of quarks and gluons in a fast nucleus may be estimated by convoluting the quark and gluon distributions in nucleons that were extracted from deep-inelastic leptoproduction from isolated nucleons with the momentum distribution of the nucleons inside a fast nucleus.

The momentum distribution of nucleons in a nucleus that moves with a relativistic velocity cannot be extracted from its nonrelativistic wave function. In fact, a knowledge of this distribution requires the solution of a complicated relativistic quantum-mechanical many-body problem. Solutions of such relativistic bound-state problems have not been found yet. Instead, attempts were made to determine these distributions by extracting the leading behavior from the lowest-order diagrams in perturbation theory.[6] The following "counting rules" were obtained: If one denotes by x_{NA} the fraction of the total momentum of a nucleus A that is carried by a single nucleon N inside a fast nucleus, then for large values of x_{NA} its momentum distribution behaves like

$$N_A(x_{NA}) \sim (1 - x_{NA})^{2T(A-1)-1},$$

where T depends upon the basic nucleon-nucleon interaction; $T=1$ for a renormalizable interaction between the nucleons, such as a vector exchange with point interactions; $T=3$ for a nucleon-nucleon interaction which is mediated by the exchange of vector mesons with a monopole form factor at each vertex, etc. Although initially the counting rules with $T=3$ were shown to correctly describe the fragmentation of certain relativistic heavy ions, it was soon realized that they cannot describe the fragmentations of nuclei heavier than carbon.[7] The powers observed in backward production of fragments from heavy nuclear targets by high-energy incident protons are much smaller than those predicted with either $T=1$ or $T=3$. These counting rules are also in conflict with many other deep-inelastic production experiments from nuclear targets.[1]

However, the counting rules were obtained under the assumption that the nucleus is fully broken up (into A nucleons for $T=1$, and into $3A$ valence quarks for $T=3$) during the collision. Such an assumption may be reasonable for high-energy central (small impact-parameter) nucleus-nuclues collisions, or for high-energy particle collisions with very light nuclei, but it is unreasonable and in conflict with experimental observations in collisions between high-energy particles and medium and heavy nuclei. The multiplicity distribution of charged nuclear fragments in such collisions was studied extensively by emulsion techniques. It was found to be energy independent and to drop rapidly with increasing number of nuclear fragments.[8]

We propose to replace the nuclear counting rules of Blankenbecler and Schmidt[6] by more realistic, and yet simple, nulcear counting rules. We note that when a nucleus is viewed from a high-momentum frame it is Lorentz contracted. All its nucleons that lie within an imaginary tube with a nucleon cross section σ, which is drawn along the momentum axis, are contracted into a small volume with the same cross section. Owing to the shortening of longitudinal dimensions all the quarks in the contracted tube will now communicate easily via exchange of massless gluons, while their communication in the transverse direction will not be affected. Lorentz contraction will simultaneously increase the longitudinal momentum components of the quarks due to the uncertainty principle and reduce the strength of their interactions due to asymptotic freedom.[9] Thus the quarks in a Lorentz-contracted tube will behave like a free Fermi gas, except for clustering of quarks into weakly interacting nucleons which reduces their total Fermi energy. The total momentum of the tube will therefore be distributed among its constituent nucleons according to phase-space rules which we shall derive below.

Let us denote by p_q, p_N, and p_t, respectively, the momenta of a quark, of a nucleon, and of a tube in a nucleus that is viewed in a high-momentum frame and let us also define fractional mo-

mentum variables through

$$x_{qN}=p_q/p_N,\quad x_{Nt}=p_N/p_t,\quad x_{qt}=p_q/p_t=x_{qN}\,x_{Nt}\,.$$

We shall first assume that the structure functions of quarks in nucleons and of nucleons in nuclei obey Bjorken scaling.[4] (Scaling violations that are implied by QCD will be introduced at a later stage.) If quarks are confined to nucleons in a tube, then their momentum distribution in a tube is given by

$$q_t(x)=\int_0^1\int_0^1 q_N(x_{qN})N_t(x_{Nt})\delta(x-x_{qN}\,x_{Nt})dx_{qN}\,dx_{Nt}\,, \tag{2.1}$$

i.e.,

$$q_t(x)=\int_x^1 q_N(x')N_t\left(\frac{x}{x'}\right)\frac{dx'}{x'}, \tag{2.2}$$

where $x\equiv x_{qt}$ and $x'\equiv x_{qN}$. $q_N(x')$ is the momentum distribution of quarks of type q in a nucleon and $N_t(x_{Nt})$ is the momentum distribution of nucleons in a tube. They satisfy the normalization conditions

$$\int_0^1 q_N(x)dx=i_q(N)\,, \tag{2.3}$$

$$\int_0^1 N_t(x)dx=i_N(t)\,, \tag{2.4}$$

where $i_q(N)$ is the number of quarks of type q in a nucleon and $i_N(t)\equiv i$ is the number of nucleons in the tube. Since we assume that the nucleons in a tube carry almost all its momentum (because it is colored, a single gluon cannot be exchanged between colorless nucleons) we have also the approximate sum rule

$$\int_0^1 xN_t(x)dx=1\,. \tag{2.5}$$

$q_N(x)$ are known from deep-inelastic scattering of leptons on nucleons. For instance, $u_N(x)$ and $d_N(x)$ can be represented (modulo scaling-violating logarithmic corrections) by

$$u_p(x)=d_N(x)=\frac{36}{16}\frac{(1-x)^3}{\sqrt{x}}, \tag{2.6}$$

$$d_p(x)=u_n(x)=\frac{315}{256}\frac{(1-x)^4}{\sqrt{x}}\,. \tag{2.7}$$

From our previous arguments it follows that a reasonable choice for $N_t(x)$, the fractional momentum distribution of nucleons inside a tube, is the relative phase space of a single nucleon carrying a fraction x of the total momentum of i identical nucleons uncorrelated except for energy (longitudinal momentum) conservation. The phase-space density $P(x)$ for such a nucleon is given by

$$P(x)dx=\int_{i-1}\cdots\int_1\prod_{j=1}^{i}\frac{d^3p_j}{2E_j}\delta\Big(E-E_i-\sum_{k=1}^{i-1}E_k\Big)\,, \tag{2.8}$$

where

$$E-E_i\simeq E-xE=(1-x)E\,.$$

In Appendix A we show that Eq. (2.8) yields

$$N_t(x)=\frac{iP(x)}{\int P(x)dx}\simeq i(2i-1)(2i-2)x(1-x)^{2i-3}\,. \tag{2.9}$$

This choice of $N_t(x)$ automatically satisfies the normalization condition (2.4) and the momentum sum rule (2.5). It also follows from the dimensional-counting rules of Blankenbecler and Brodsky,[10] combined with conditions (2.4) and (2.5), or if the interaction between the nucleons in a tube is described by a field theory with a renormalizable interaction such as $\lambda\phi^4$, vector exchange, etc.[6]

We now substitute Eqs. (2.6), (2.7), and (2.9) into (2.2) and obtain the structure functions of quarks in a tube of i *protons*:

$$\tilde{u}_i(x)=\frac{36}{16}\frac{3}{2i+1}\frac{(1-x)^{2i+1}}{\sqrt{x}}\times F(2.5,2i-2,2i+2;1-x)\,, \tag{2.10}$$

$$\tilde{d}_i(x)=\frac{315}{256}\frac{12}{(2i+1)(2i+2)}\frac{(1-x)^{2i+2}}{\sqrt{x}}\times F(3.5,2i-2,2i+3;1-x)\,. \tag{2.11}$$

Similarly, since by isospin invariance $d_n=u_p$ and $u_n=d_p$, where n stands for neutron, for a tube that contains $(Z/A)i$ protons and $[(A-Z)/A]i$ neutrons we obtain

$$u_i(x)=(Z/A)\tilde{u}_i(x)+[(A-Z)/A]\tilde{d}_i(x)\,, \tag{2.12}$$

$$d_i(x)=(Z/A)\tilde{d}_i(x)+[(A-Z)/A]\tilde{u}_i(x)\,. \tag{2.13}$$

$F(a,b,c;z)$ in Eqs. (2.10) and (2.11) is the confluent hypergeometric function, represented by the integral

$$F(a,b,c;z)=\frac{1}{B(b,c-b)}\int_0^1 t^{b-1}(1-t)^{c-b-1}(1-tz)^{-a}dt\,, \tag{2.14}$$

where

$$B(u,v)=\frac{\Gamma(u)\Gamma(v)}{\Gamma(u+v)}\,. \tag{2.15}$$

In general, for any type of parton q in a nucleon N, with a structure function of the form

$$q_N(x)=C_q x^{\alpha}(1-x)^{\beta}, \tag{2.16}$$

we obtain

$$q_i(x)=q_N(x)i(2i-1)(2i-2)(1-x)^{2i-2}B(2i-2,\beta+1)$$
$$\times F(\alpha+\beta,2i-2,2i+\beta-1;1-x). \tag{2.17}$$

C_q in Eq. (2.16) is a constant which for valence quarks equals $i_q(N)/B(\alpha+1,\beta+1)$, $i_q(N)$ being the number of q-type quarks in the nucleon. The quark distributions (2.10), (2.11), and (2.17) for sea quarks and gluons are illustrated in Fig. 1.

Note that $F(a,b,c;0)=1$ [provided that $\mathrm{Re}(c-a-b)\geq 0$], and thus for $x\to 1$,

$$\tilde{u}_i(x)\sim(1-x)^{2i+1}. \tag{2.18}$$

The power $2i+1$ can be obtained directly from the dimensional-counting rules[10] if one assumes that the elementary spectators accompanying a valence quark in a nucleon are the two other valence quarks in the hit nucleon and all the other nucleons in the tube [i.e., $n_s=2+(i-1)$ and thus $2n_s-1=2i+1$].

The quark distributions (2.10), (2.11), and (2.17) in nuclei are considerably different from the corresponding distributions (2.6), (2.7), and (2.16) in isolated nucleons. As a consequence production processes which depend on quark distributions in the target exhibit a nontrivial A dependence. Moreover, the distributions yield a considerable probability for a quark in a nucleus to carry momentum much larger than the average momentum per nucleon in the nucleus (see Fig. 1). Such momenta lead to subthreshold production of particles and to cumulative production of particles,[11] i.e., to production of masses and momenta which cannot be produced in collisions between isolated nucleons. We shall make explicit use of the quark distributions (2.10), (2.11), and (2.17) in our calculations of production processes that do depend on quark distributions. Thus in such processes the explicit quark distributions will replace the "universality assumption" of the collective tube model.[12]

We stress again that neither the off-shell momentum distributions of quarks in a nucleon at rest nor their off-shell momentum distributions in a nucleus at rest are related in any simple way (e.g., via Lorentz transformations) to the corresponding distributions in fast nucleons and in fast nuclei.

The probability that a nucleon in a nucleus is found in a tube of i nucleons can be estimated in the following way[12]: Let us assume that the nuclear wave function can be well approximated by a product of A identical nucleon wave functions. Then the probability of finding a nucleon inside a tube of cross section σ at impact parameter b is $\sigma T(b)/A$, where $T(b)$ is the nuclear thickness at impact parameter b:

$$T(b)=\int_{-\infty}^{\infty}|\psi(b,z)|^2dz=\int_{-\infty}^{\infty}\rho(b,z)dz. \tag{2.19}$$

$\rho(b,z)\equiv|\psi(b,z)|^2$ is the nuclear density at (b,z) normalized such that $\int\rho(b,z)d^3r=A$. The probability of finding i out of A nucleons inside a tube of cross section σ at impact parameter b is thus given by

$$P(i,a;b)=\binom{A}{i}\left(\frac{\sigma T(b)}{A}\right)^i\left(1-\frac{\sigma T(b)}{A}\right)^{A-i} \tag{2.20}$$

and the probability of finding a tube of i nucleons at any impact parameter is

$$P(i,A)=\int P(i,A;b)d^2b\Big/\sum_{i=1}^{A}\int P(i,A;b)d^2b, \tag{2.21}$$

where

$$\int\sum_{i=1}^{A}P(i,A;b)d^2b=\int\left[1-\left(1-\frac{\sigma T(b)}{A}\right)^A\right]d^2b. \tag{2.22}$$

The nuclear density functions $\rho(r)$ can be extracted from experimental data on low-energy electron scattering on nuclei. $P(i,A)$ for a representative set of nuclei are listed in Appendix B.

Equipped with quark distributions in fast nuclei and with the probability distributions $P(i,A)$ we can now proceed to calculate specific cross sections in high-energy lepton-nucleus and hadron-nucleus collisions.

III. DEEP-INELASTIC LEPTON SCATTERING FROM NUCLEI

Our quark-parton model of the nucleus can be tested directly in deep-inelastic lepton scattering from nuclei. Consider first scattering of an unpolarized e/μ beam from unpolarized target particles of mass M in the one-photon exchange approximation. The energy E of the incident lepton, the energy E' of the scattered lepton, and its scattering angle define completely the virtual photon whose four momentum $q=(\nu,\vec{q})$ is given by

$$-q^2=4EE'\sin^2(\theta/2), \tag{3.1}$$

$$\nu=E-E'. \tag{3.2}$$

In terms of the Bjorken scaling variables $x\equiv -q^2/-q_{\max}{}^2=-q^2/2M\nu$ and $y\equiv\nu/E$, the double-differential cross section for inelastic scattering can be written as

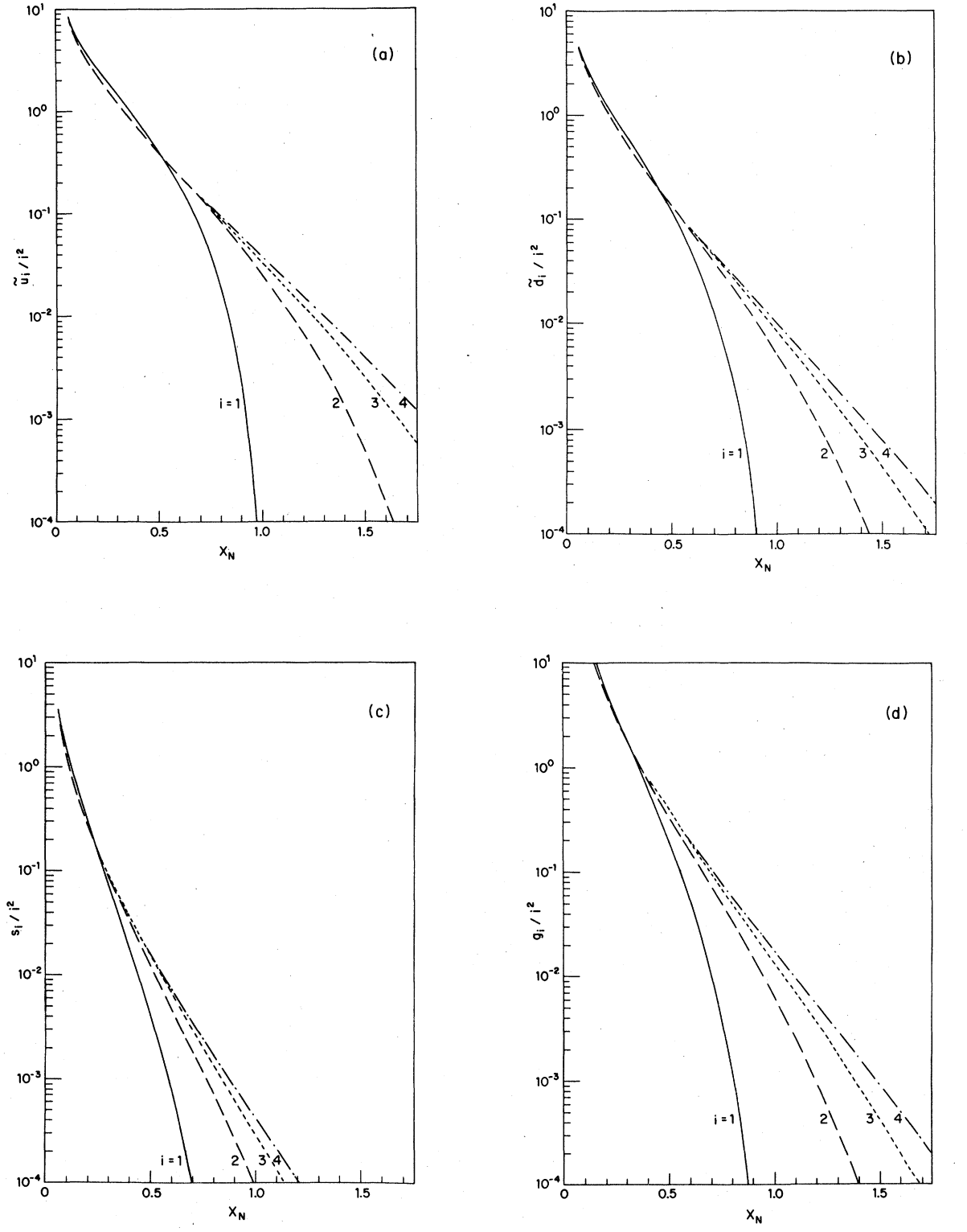

FIG. 1. The x distribution of (a) u quarks, (b) d quarks, (c) sea quarks, and (d) gluons in a proton in a tube that consists of $i=1$, 2, 3, 4 protons, viewed in a high-momentum frame. u_p, d_p, s_p, and g_p are given respectively, by the parametrizations (2.6), (2.7), and (2.16) with $\alpha=-1$, $\beta=7$, and $C_s=0.25$ for sea quarks and $\alpha=-1$, $\beta=5$, and $C_g=3.50$ for gluons.

$$\frac{d^2\sigma}{dx\,dy}=\frac{8\pi\alpha^2 ME}{q^4}\left[\left(1-y-xy\frac{M}{2E}\right)F_2(x,q^2)+\frac{y^2}{2}2xF_1(x,q^2)\right]. \tag{3.3}$$

The naive quark-parton model obeys exact Bjorken scaling[4]:

$$F_i(x,q^2)=F_i(x)\,; \tag{3.4}$$

it satisfies the Callan-Gross relation[13]

$$F_2(x)=2xF_1(x)\,, \tag{3.5}$$

and in the high-energy limit it yields

$$\frac{d^2\sigma}{dx\,dy}=\frac{8\pi\alpha^2 ME}{q^4}(1-y+y^2/2)F_2(x)\,, \tag{3.6}$$

where

$$F_2(x)=\sum_q x e_q^{\,2} q(x)\,, \tag{3.7}$$

e_q is the charge of the quark q, $q(x)$ is its x distribution in the target particle, and the summation extends over all quark flavors in the target particle. The existence of a significant diquark substructure in the nucleon will lead to violation of both the Callan-Gross relation and Bjorken scaling. In Sec. VI we will show strong evidence for its existence.

Quark flavors other than u,d,s do not contribute significantly to $F_2(x)$ of nucleons and of nuclei. We shall neglect their contribution as well as QCD scaling-violating corrections to $F_2(x)$ of nuclei. We also note that for a tube of i nucleons $M=im$, where m is the nucleon mass and

$$x_i=-q^2/2M\nu=-q^2/2im\nu=x_N/i\,. \tag{3.8}$$

Consequently for a nucleus we can write

$$F_2(x_N)=\frac{\sigma^A}{\sigma}\sum_{i=1}^{A}P(i,A)\,x_i\left[\tfrac{4}{9}(u_i+\bar{u}_i)+\tfrac{1}{9}(d_i+\bar{d}_i+s_i+\bar{s}_i)\right], \tag{3.9}$$

where all the structure functions in (3.9) are evaluated at $x_i=x_N/i$ according to expressions (2.10)–(2.17). σ^A/σ is the average number of nuclear tubes as seen by the virtual photon (σ^A, σ are total inelastic pA,pp cross sections, respectively) and $P(i,A)$, the probability that a nuclear tube contains exactly i nucleons, is given by expressions (2.20)–(2.27). $P(i,A)$ for various nuclei are listed in Table I in Appendix B.

In our calculations of $F_2(x_N)$ for nuclei we have used the approximate parametrizations (2.6) and (2.7) of, respectively, u_p and d_p. We have also assumed an SU(3)-symmetric sea, $\bar{u}_i=\bar{d}_i=\bar{s}_i=s_i$, with $\alpha=-1$ (Regge behavior), $\beta=7$ (dimensional-counting rules[20]), and $C_q=0.25$ (corresponds to $\langle x_{\rm sea}\rangle=0.19$ as determined from deep-inelastic neutrino and antineutrino scattering[14]).

Since our parametrization of the nucleon structure functions are only approximate and since they ignore scaling-violating QCD corrections, we expect our calculations to yield only an approximate description of the nuclear structure functions. However, we do expect that our predictions yield a more accurate description of the A dependence of the nuclear structure functions, because the A dependence is not very sensitive to the exact parametrization of the nucleon structure functions and because scaling-violating QCD corrections are insensitive to A (due to the fact that color singlet nucleons cannot exchange single gluons).

In Fig. 2 we present our predictions for the A dependence of $F_2(x_N)$. As can be seen from Fig. 2 for $x_N\leq 0.5$ the A dependence is not much different from the "naive" A^1 dependence. However, our model predicts a strong enhancement of the nuclear structure functions beyond $x\sim 0.5$, which increases rapidly with x_N. Note in particular that while we predict nuclear structure functions which do not vanish beyond $x_N=1$, the naive model predicts nuclear structure functions that behave like A^1 and vanish beyond $x_N=1$.

Experimental data on the A dependence of inelastic e/μ scattering from nuclei was published by two separate groups.[15] In Fig. 3 we compare these data and our theoretical predictions for α

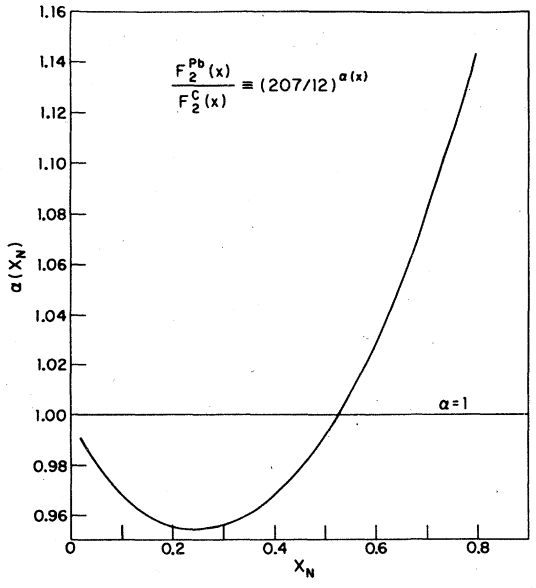

FIG. 2. The A dependence of the ratio $R(\mathrm{Pb/C})\equiv F_2^{\mathrm{Pb}}/F_2^{\mathrm{C}}$ as function of x_N. $\alpha(x_N)$ is defined through $R(A_2/A_1)=(A_2/A_1)^{\alpha(x_N)}$. $F_2^A(x_N)$ were calculated from expression (3.9) as explained in the text.

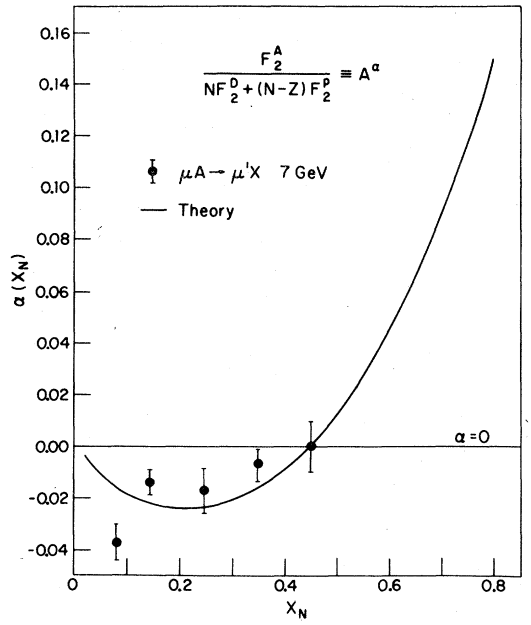

FIG. 3. Comparison between experimental results on the A dependence of nuclear structure functions derived from deep-inelastic scattering of 7-GeV muons on nuclear targets, and the A dependence predicted by the quark-parton model of the nucleus as given by expression (3.9). The comparison is presented in terms of the parameter $\alpha(x_N)$ defined by Eq. (3.10).

which is defined through

$$\frac{F_2^A}{NF_2^D+(N-Z)F_2^p}=A^\alpha . \tag{3.10}$$

As can be seen from Fig. 3, the theoretical predictions are consistent with the experimental data, except at $x_N=0.147$. This discrepancy may reflect the low q^2 of the measurements.

Accurate experimental data on nuclear structure functions at $x_N>0.5$, and in particular $x_N>1$, derived from deep-inelastic scattering of leptons on nuclear targets will be extremely useful for testing our model, as well as other theoretical models of complex nuclei viewed in high-momentum frames.

IV. LEPTON PAIR PRODUCTION OFF NUCLEAR TARGETS

Heavy μ pairs are usually produced off nuclear targets to enhance the otherwise small production rates.[16-19] The quark-parton model of the nucleus, described in Sec. II, enables us to investigate the A dependence of these processes, namely, hadron $+A\to\mu^+\mu^-+X$ at high incident energies and large dilepton masses Q.

We shall limit ourselves to a zero-order calculation of the Drell-Yan[19] mechanism, where a parton from the projectile and its antiparton from the target annihilate into a massive virtual photon, which subsequently decays into a μ pair. (First-order QCD scaling-violation corrections will be treated in a forthcoming publication).

Consider a massive lepton pair produced in a hadron-proton collision $h+p\to\mu^+\mu^-+X$. The mass of the pair is given by the sum of their four-momenta squared:

$$Q^2=(p_{\mu^+}+p_{\mu^-})^2 . \tag{4.1}$$

It is customary to define the scaled variable

$$\tau=Q^2/s,\quad s\simeq 2mp_{\rm LAB}, \tag{4.2}$$

where s is the c.m. energy squared, m is the proton mass, and $p_{\rm LAB}$ is the incident momentum.

The Drell-Yan cross section for the production of a μ pair of mass Q is given by the formula[19]

$$\frac{d\sigma^{hp\to\mu^+\mu^-+X}}{dQ}=\frac{1}{3}\frac{8\pi\alpha^2}{3Q^3}\int\frac{dx_1}{x_1}\sum_q \bar q_h(x_1)q_p(x_2)\Big|_{x_2=\tau/x_1} . \tag{4.3}$$

In (4.3) the factor of $\frac{1}{3}$ is due to color, α is the fine-structure constant, q_h and q_p are parton distributions in the incident hadron and the target proton, respectively, and the sum extends over all quark types, valence and sea.

In the following calculations we shall need, in addition to (2.6) and (2.7), the sea distribution in the proton and all quark distributions in a pion. We include in the calculations only light quarks, up, down, and strange, and assume an SU(3)-symmetric sea. In accordance with dimensional-counting rules[10,20] and with the fact that gluons in the proton carry about half its momentum we obtain

$$u_p^s(x)=\bar u_p(x)=d_p^s(x)=\bar d_p(x)$$
$$=s_p(x)=\bar s_p(x)\equiv\xi_p(x), \tag{4.4}$$

$$\xi_p(x)=\frac{0.25}{x}(1-x)^7 . \tag{4.5}$$

Similar considerations yield the following pion quark distributions. We have for valence quarks:

$$u_{\pi^+}=d_{\pi^+}=d_{\pi^-}=\bar u_{\pi^-}=v_\pi ,$$
$$v_\pi(x)=\frac{3}{4}\frac{(1-x)}{\sqrt{x}}; \tag{4.6}$$

and for all sea quarks:

$$\xi_\pi(x)=\frac{0.1}{x}(1-x)^5 . \tag{4.7}$$

The passage from hp collisions to hA collisions is carried out in two steps.

Step 1. Derivation of the production cross section for the process

$$h + \text{tube}(i) \to \mu^+\mu^- + X .$$

Consider the production of a μ pair by an incident hadron h on an average i nucleon tube, containing $i(Z/A)$ protons and $i[(A-Z)A]$ neutrons. The cross section for the production of a lepton pair can be obtained from Eq. (4.3) by the replacement

$$q_p(x_2=\tau/x_1) \to q_i(x_2=\tau/ix_1) , \tag{4.8}$$

hence

$$\frac{d\sigma^{h+i\to\mu^+\mu^-+X}}{dQ} = \frac{1}{3}\frac{8\pi\alpha^2}{3Q^3}\int \frac{dx_1}{x_1}\sum_q \bar{q}_h(x_1)q_i(x_2)\Big|_{x_2=\tau/ix_1} \tag{4.9}$$

The transformation $x_2=\tau/x_1 \to x_2=\tau/ix_1$ reflects the fact that x_2, the fraction of momentum carried by the target parton, is a fraction of the momentum of the whole nuclear tube, rather than of the average momentum of a single nucleon. Specifically,

$$\begin{aligned} &u_p(\tau/x_1) \to u_i(\tau/ix_i) + \xi_i(\tau/ix_1) , \\ &d_p(\tau/x_1) \to d_i(\tau/ix_i) + \xi_i(\tau/ix_1) , \\ &(\bar{u}_p, \bar{d}_p, s_p, \bar{s}_p)\big|_{x_2=\tau/x_1} \to \xi_i(\tau/ix_1) , \end{aligned} \tag{4.10}$$

where $\xi_i(x)$ is obtained from Eqs. (4.5) and (2.17) with $\alpha=-1$ and $\beta=7$, and $u_i(x)$ and $d_i(x)$ are given, respectively, by Eqs. (2.12) and (2.13).

The limit of the x_1 integration is fixed by baryon-number conservation. Thus $(p_p+p_i-Q)^2 \geq [m(i+1)^2]$ for $p+\text{tube}(i) \to \mu^+\mu^-+X$ and $(p_\pi+p_i-Q)^2 \geq (im)^2$ for $\pi+\text{tube}(i) \to \mu^+\mu^-+X$. At $p_{\text{LAB}} \to \infty$ both inequalities reduce to $\tau/i \leq x_1 \leq 1$. In the derivation of the theoretical predictions as presented in Figs. 4–6 we follow the experimental procedure and integrate x_1 over the limited interval $x_F \equiv x_1 - ix_2 = x_1 - \tau/x_1 \geq 0$, i.e., $x_1 \geq \sqrt{\tau}$.

Step 2. Averaging over all possible tubes in the nucleus A. This step is carried out as follows:

$$\frac{d\sigma^{hA\to\mu^+\mu^-+x}}{dQ} = \frac{\sigma^A}{\sigma}\sum_{i=1}^{A} P(i,A)\frac{d\sigma^{h+i\to\mu^+\mu^-+X}}{dQ} . \tag{4.11}$$

In (4.11) $P(i,A)$ is the probability of hitting a tube of exactly i nucleons in an encounter with the nucleus A. Its explicit form is given by (2.19)–(2.22). The factor σ^A/σ is the average number of independent tubes, each of cross section σ in the nucleus A, contributing additively to the nuclear production rate.

Equations (4.9) and (4.11) summarize our predictions for the nuclear Drell-Yan cross section. We have compared our predictions with the experimental data on $\pi^-A \to \mu^+\mu^-+X$ of Anderson *et al.*[21] and with the experimental data on $pA \to \mu^+\mu^-+X$ of Kaplan *et al.*[22] The results are presented in Figs. 4–6.

In Fig. 4 we compare the theoretical cross section per nucleon

$$\frac{1}{A}\frac{d\sigma^{\pi^-A\to\mu^+\mu^-+X}}{dQ}$$

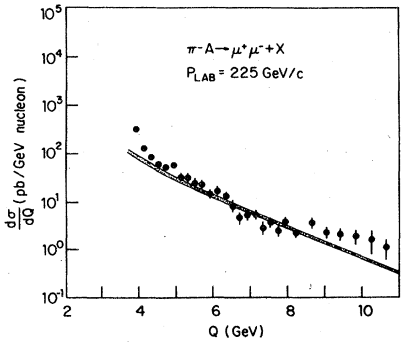

FIG. 4. Comparison between experimental results (Ref. 21) and our theoretical predictions for the dependence of the cross section per nucleon $(1/A)\sigma(\pi^-A \to \mu^+\mu^-+X)$ on the dilepton mass at $p_{\text{LAB}}=225$ GeV/c.

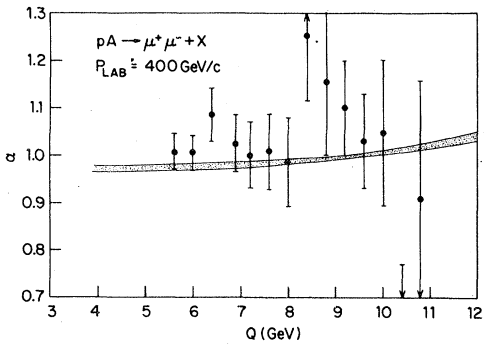

FIG. 5. Comparison between experimental results (Ref. 22) and our theoretical predictions for α_{12} as defined by Eq. (4.12) for $pA \to \mu^+\mu^-+X$ at $p_{\text{LAB}}=400$ GeV/c. The finite width of the theoretical line reflects the dependence of α_{12} on A_1 and A_2.

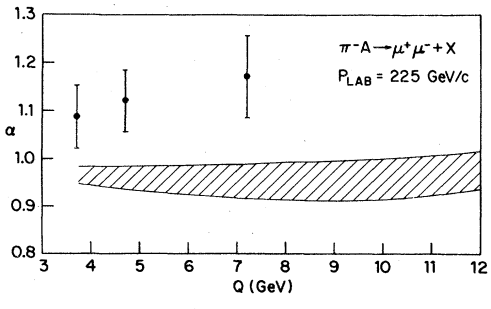

FIG. 6. Comparison between experimental results (Ref. 21) and our theoretical predictions for α_{12} as defined by Eq. (4.12) for $\pi^-A \to \mu^+\mu^-+X$ at $p_{\text{LAB}}=225$ GeV/c. The width of the line reflects the dependence of α_{12} on the choice of A_1 and A_2.

and the experimental data of Ref. 21. The finite width of the theoretical line is due to the fact that different nuclear targets yield theoretically slightly different cross sections per nucleon. This figure shows that our choice of structure function is in satisfactory agreement with the experimental data, both in shape and magnitude.

Let us now consider the A dependence of lepton pair production and let us define the quantity α_{12} through

$$R(A_1/A_2) = \sigma_{h+A_1\to\mu^+\mu^-+X}/\sigma_{h+A_2\to\mu^+\mu^-+X} = (A_1/A_2)^{\alpha_{12}}. \quad (4.12)$$

Obviously a naive parton model where a parton carries only a fraction of the average momentum per nucleon in a nucleus would predict $R(A_1/A_2) = A_1/A_2$, i.e., $\alpha_{12}=1$ for all Q values. Our model, on the other hand, gives a nontrivial A dependence. In Fig. 5 we compare our predictions for α_{12} and experimental results[22] on $pA\to\mu^+\mu^-+X$ at $p_{\mathrm{LAB}} = 400$ GeV/c. The finite width of the theoretical predictions reflect the dependence of α_{12} on the choice of A_1 and A_2. The experimental data are consistent with our predictions, but statistics are not good enough to identify small deviations of α_{12} from 1. In Fig. 6 we compare our predictions for α_{12} and experimental results[21] on $\pi^-A\to\mu^+\mu^-+X$ at $p_{\mathrm{LAB}} = 225$ GeV/c. As can be seen from Fig. 6, the theoretical predictions are below the experimental data points. However, the A dependence and/or the normalization of these data is inconsistent with new data on $\pi A\to\mu^+\mu^-+X$.[23]

In Figs. 7(a) and 7(b) we present our predictions of α_{12} for Ta/C, Ta/Cu, and Cu/C as a function of τ for, respectively, $\pi^-A\to\mu^+\mu^-+X$ and $pA\to\mu^+\mu^-+X$. As can be seen from these figures, we predict large deviations from the naive predictions $\alpha=1$, especially at large τ values in pA collisions.

Although our detailed predictions depend on the specific parametrizations that we have chosen for the quark distributions in nucleons and in mesons, the A dependence that we predict is not very sensitive to the specific choices. High-statistics experimental data on the A dependence of lepton pair production at large values of τ will therefore be of extreme interest.

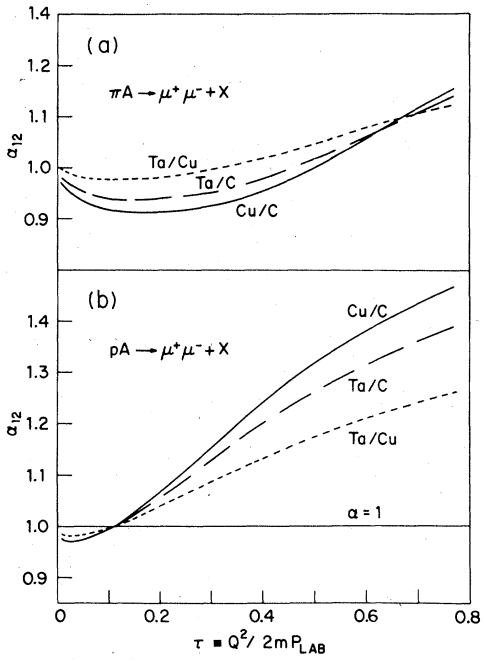

FIG. 7. Theoretical predictions of α_{12} as function of τ for Ta/C, Cu/C, and Ta/Cu for, respectively, (a) $\pi^-A\to\mu^+\mu^-+X$ and (b) $pA\to\mu^+\mu^-+X$.

V. PRODUCTION OF W BOSONS OFF NUCLEAR TARGETS

The unified electroweak theory of Weinberg and Salam[24] has been recently tested successfully in various experiments, and apparently it is well on its way to becoming the theory of electromagnetic and weak processes. It is, therefore, of great importance to establish experimentally the existence of the mediators of the weak force, the intermediate vector bosons $W^\pm$ and Z, which are the cornerstones of this theory. The energy of the currently operating accelerators is below the threshold energy for their production. The W mass is predicted to be

$$m_W = 37.5\ \mathrm{GeV}/\sin\theta_W, \quad (5.1)$$

where θ_W is the Weinberg angle. The present best value for θ_W is $\sin^2\theta_W = 0.23\pm0.01$, fixing the W mass around 80 GeV. Thus, the production of W bosons in hadron-hadron collisions will have to wait for the next generation of accelerators such as ISABELLE at Brookhaven, the antiproton-proton collider at CERN, and the few-TeV fixed-target machine planned in the Soviet Union.

However, past experience shows that "subthreshold production" of heavy objects is not entirely impossible. In fact the antiproton was first produced "below threshold" by protons incident on a nuclear target,[25] and was explained as an energy enhancement effect due to the collective (Fermi) motion of nucleons in the target nucleus. Our quark-parton model of a fast nucleus has such a collective enhancement, due to the fact that a single parton can carry an energy exceeding the average energy per nucleon. There are clear indications that production processes from nuclear targets near or beyond the kinematic boundary of hadron-proton collision are strongly enhanced. One such example is the backward cumulative par-

ticle production[11] which is discussed in detail in Sec. VII. Another is the abnormal nuclear enhancement of high-transverse-momentum hadronic production, first observed by Cronin and his collaborators[27] in 1975, and since rediscovered in several other experiments of hadron and hadronic-jet production.[1] It is therefore possible that the use of nuclear targets may enable us to produce W bosons at "subthreshold energies" with a machine such as the energy doubler/saver at Fermilab. Here we revise our previous estimates[26] of W production from nuclear targets using our new nuclear structure functions which are described in Sec. II.

As in Sec. IV we shall confine ourselves to the calculation of the W-boson production cross section in the Drell-Yan approximation.[20] This cross section for hadron-proton collisions is given by

$$\sigma(h+p\to W^{\pm}+X)=\frac{\sqrt{2}}{3}\pi G_F[\cos^2\theta_C H_{\pm}(\tau)+\sin^2\theta_C F_{\pm}(\tau)]\,, \tag{5.2}$$

where $G_F\simeq 10^{-5}/m_p{}^2$ is the weak coupling constant, $\theta_C\simeq 0.23$ is the Cabbibo angle, and

$$\begin{aligned} H_+ &= \int \frac{dx_1}{x_1}[x_1u_h(x_1)x_2\bar{d}_p(x_2) \\ &\quad + x_1\bar{d}_h(x_1)x_2u_p(x_2)]_{x_2=\tau/x_1}\,, \\ F_+ &= \int \frac{dx_1}{x_1}[x_1u_h(x_1)x_2\bar{d}_p(x_2) \\ &\quad + x_1\bar{s}_h(x_1)x_2u_p(x_2)]_{x_2=\tau/x_1}\,, \\ H_- &= H_+(q\to\bar{q}),\quad F_- = F_+(q\to\bar{q})\,. \end{aligned} \tag{5.3}$$

The W-boson production off a nuclear target A is obtained from Eqs. (5.2) and (5.3) by the substitutions (2.10), (2.11), and (2.17). The quantity one expects to detect as a signature of W-boson production is σB, where σ is the W-boson production cross section and B is the branching ratio for the decay $W\to\mu\nu$. We have plotted σB as a function of $\tau^{-1}=2mp_{\rm LAB}/m_W{}^2$ in Fig. 8 for the processes

$$h+{}^{238}\mathrm{U}\to W\to\mu\nu+x\,,$$

where $h=\pi^+$, $\bar{p}$, and p beams, and examined the prospect of producing W bosons with the currently constructed energy saver/doubler at Fermilab.

According to Halzen and McIntire[28] a rate of one event per hour would correspond to

$\sigma B = 5\times 10^{-39}$ cm^2/nucleus for a proton beam

$= 8\times 10^{-36}$ cm^2/nucleus for a π^+ beam, and

$= 3\times 10^{-34}$ cm^2/nucleus for an antiproton beam.

For a W-boson mass around $m_W=80$ GeV and an incident beam momentum of about 1 TeV/c only a π^+ beam provides a reasonable chance of observing W bosons at a rate of about one event per week.

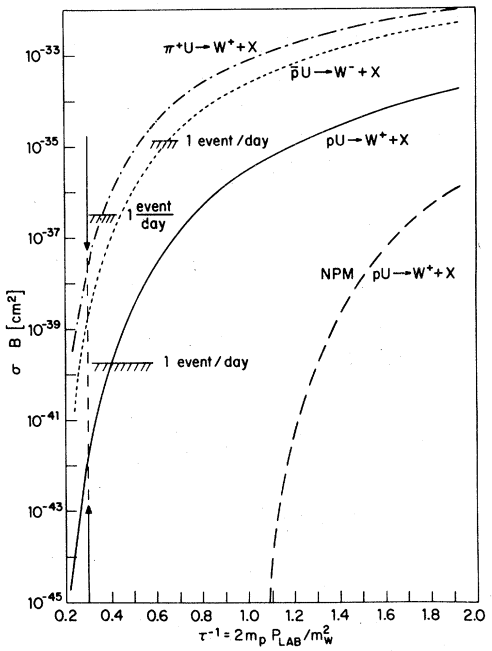

FIG. 8. Theoretical predictions of σB for the process $h+{}^{238}\mathrm{U}\to W(\to\mu\nu)+X$ where $h=p$, π, and $\bar{p}$. Only the π^+ provides an observable rate of W^+ production at the Fermilab energy saver/doubler machine, of about 1 event per week.

We stress, however, that our predictions are based on our present knowledge of nucleon and meson structure functions and they ignore scaling-violating QCD corrections. Better parameterization of nucleon and meson structure functions and inclusion of higher-order QCD corrections can slightly modify our predictions. It is important to notice that our prediction is larger than a Fermi-motion effect[28] (using the form appropriate for production below threshold).

VI. PRODUCTION OF PARTICLES WITH SMALL p_T AND LARGE x ON NUCLEI

Production of particles with small p_T and large x from nuclear targets by high-energy hadrons is not sensitive to the detailed quark-parton structure of the nucleus. Thus it cannot provide a sensitive test for our quark-parton model of the nucleus. Nevertheless, we shall discuss it here for the sake of completeness and as an introduction to cumulative backward production from nuclear targets which is very sensitive to the quark-parton structure of the nucleus and which we will discuss in Sec. VII. We will also demonstrate here the usefulness of nuclear targets in enhancing certain production channels and in filtering out specific

components of the wave function of the incident hadrons.

As is well known, soft processes in QCD require a nonperturbative approach which is still lacking. Nevertheless, attempts have been made to understand low-p_T–large-x production from nucleons in terms of the quark-parton model of the nucleon.[5] Here we shall show that the general picture underlying the qualitative successes of quark models is sufficient for obtaining a successful quantitative description of the A dependence of particle production from nuclear targets at low p_T and large x. In particular we shall show that the quark-parton model can be used to predict remarkably well the A dependence of the nuclear attenuation that was observed in nondiffractive production of hadrons with large x and small p_T by high-energy leptons[29] and hadrons[30] incident on nuclear targets. (Note however, that it has been recently observed that sometimes inclusive production of certain particles with very small p_T and large x from very heavy nuclei is strongly enhanced[31] rather than being suppressed. This is due to the excitation of the projectile by the Coulomb field of the target nucleus.[32])

The ideas that are presented below are extensions of ideas that were presented in Refs. 33–35. Following Refs. 33–35 we adopt the following quark picture of production of hadrons with large x and small p_T by high-energy incident hadrons. A fragmentation of an incident hadron occurs when one of its constituents collides with a target nucleon. Its other constituents can either escape inelastic collisions within the target and retain their original fractions x of the incident momentum (we shall call them spectators) or suffer collisions which change their nature and/or momentum. The constituents hadronize by fragmentation and recombination with other constituents newly produced or already present in the target or in the projectile. We first argue that hadrons with large x are mainly produced through the fragmentation and recombination of the valence quarks of the projectile. From deep-inelastic lepton scattering we know that the x distribution of sea quarks decreases rapidly with increasing x values and, except for very small values of x, it is much smaller than the x distribution of valence quarks. This is illustrated in Fig. 1 where we have compared $u_p(x)$, $d_p(x)$, $\bar{u}_p(x)$, and $\bar{d}_p(x)$ as given by formulas (2.6), (2.7), and (2.9), and $g_p(x)$, the x distribution of gluons, which is given by

$$g_p(x) = 0.25x^{-1}(1-x)^5 .$$

This choice of $g_p(x)$ satisfies the dimensional-counting rules,[10] it has the correct Regge behavior at $x \sim 0$, and it is normalized such that $\int_0^1 x g_p(x)\,dx \simeq 0.5$, which is required by the experimental data on deep-inelastic lepton scattering from nucleons.[36] At large values of x $g_p(x)$ is also very small compared with the x distribution of valence quarks. Thus as a first approximation we shall neglect the contribution from the fragmentation and recombination of gluons and sea quarks to the production of hadrons with large values of x. We shall later show that their contribution does not change our results for $x \gtrsim 0.2$. We will also show that the contribution from the fragmentation and recombination of wounded quarks,[35] i.e., of quarks that have suffered inelastic collisions while passing through the nucleus, to the formation of hadrons with large x and small p_T is small compared with that of valence quarks that have escaped collisions. We thus begin with the following approximate picture[34] for the production of hadrons with large x and small p_T.

A. Recombination of spectator quarks

During the collision valence quarks of the projectile, which escape collisions and retain their original fraction x of the incident momentum [spectator quark(s)], can hadronize by recombining with slow quark(s) ($x \approx 0$) either newly produced or already present in the target or in the beam, as in the recombination models. They may also emit slow fragments and then recombine, as in the quark fragmentation/cascade models. In both cases, the recombination results in a produced particle that has approximately the same x as that of the spectator quark(s). (We do not consider a process where all the valence quarks pass through without inelastic interactions. Such a process may contribute to elastic scattering and diffractive inelastic scattering, which are out of the scope of the present model.) These mechanisms are illustrated by the quark diagrams in Fig. 9. An important property of these diagrams is that their A and x dependence factorize: Different x dependence of the quark diagrams for different targets can come only from A-dependent momentum distributions of the target quarks (or the quarks newly produced in the central region) that recombine with the leading quarks to form the large-x hadrons. However, if we denote by x_1 and x_2 the fractional c.m. momenta of the partons (quarks, antiquarks, etc.) in the projectile and in the target, respectively, that recombine into a hadron of mass m with the fractional momentum $x = x_1 - x_2$ ($0 \leq x_i \leq 1$), then x_i ($i = 1, 2$) must satisfy

$$x_i = [(-1)^{i+1}x + (x^2 + 4m^2/s)^{1/2}]/2 ,$$

i.e.,

$$(x + x_2)x_2 = m^2/s , \tag{6.1}$$

where s is the square of the c.m. energy of the colliding particles. For large positive x values and high energies ($m^2/s \to 0$) Eq. (6.1) requires that $x_2 \to 0$, and thus $x = x_1$ and the x distribution of the hadrons produced via a particular diagram in Fig. 9 depends only on the projectile. (Note, however, that two different quark diagrams can have both different A dependence and different x dependence, as we shall see below. Consequently, processes where more than one type of quark diagrams contribute can have an A dependence that changes with x.)

Since free quarks do not seem to exist, quarks must hadronize before leaving the interaction region, and the sum of the probabilities of all the possible recombinations must be independent of A. If the relative abundance of quark flavors around $x \sim 0$ is A independent, then also the individual recombination probabilities are A independent. Hence the A dependence of the quark diagrams result only from the A dependence of the probabilities of the valence quarks of the projectile colliding with target nucleons while the projectile passes through the target nucleus. This A dependence can be calculated using standard "nuclear optics" techniques.[12] Let $S_{xA}(q_1,\ldots,q_k)$ denote the inelastic cross section for stripping the valence quarks $q_1,\ldots,q_k$ from the projectile x when it passes through the target nucleus A. Let σ_q be the quark-nucleon total cross section ($q = u,\bar{u},d,\bar{d},s,\bar{s}$, etc.) and let $T(b)$ be the nuclear thickness at impact parameter b along the incident z direction. The probability that an incident quark at impact parameter b will pass through the nucleus without collisions is $[1-\sigma_q T(b)/A]^A$ and with the aid of the optical relation

$$\sigma_{xA} = \int \{1-[1-\sigma_{xp}T(b)/A]^A\}\,d^2\vec{b} \underset{A\gg 1}{=} \int \{1-\exp[-\sigma_{xp}T(b)]\}\,d^2\vec{b} \tag{6.2}$$

and the additive-quark-model relations[37]

$$\sigma_u \simeq \sigma_d \simeq \sigma_{\bar{u}} \simeq \sigma_{\bar{d}} \simeq (\tfrac{1}{2})\sigma_{\pi p} \simeq (\tfrac{1}{3})\sigma_{pp}\,, \tag{6.3a}$$

$$\sigma_s \simeq \sigma_{\bar{s}} \simeq \sigma_{K^- p} - (\tfrac{1}{2})\sigma_{\pi^- p} \simeq \sigma_{K^+ p} - (\tfrac{1}{2})\sigma_{\pi^+ p}\,, \tag{6.3b}$$

it is easy to derive relations such as

$$\begin{aligned}
&S_{\pi A}(q) = S_{\pi A}(\bar{q}) = \sigma_{\pi A} - \sigma_{qA}\,,\\
&S_{\pi A}(q\bar{q}) = 2\sigma_{qA} - \sigma_{\pi A}\,,\\
&S_{KA}(s) = S_{KA}(\bar{s}) = \sigma_{KA} - \sigma_{qA}\,,\\
&S_{KA}(q) = S_{KA}(q) = S_{KA}(\bar{q}) = \sigma_{KA} - \sigma_{sA}\,,\\
&S_{KA}(s\bar{q}) = S_{KA}(q\bar{s}) = \sigma_{sA} + \sigma_{qA} - \sigma_{KA}\,,\\
&S_{pA}(d) = (\tfrac{1}{2})S_{pA}(u) = \sigma_{pA} - \sigma_{\pi A}\,,\\
&S_{pA}(uu) = (\tfrac{1}{2})S_{pA}(ud) = 2\sigma_{\pi A} - \sigma_{pA} - \sigma_{qA}\,,\\
&S_{pA}(uud) = \sigma_{pA} + 3\sigma_{qA} - 3\sigma_{\pi A}\,,
\end{aligned} \tag{6.4}$$

where q stands for nonstrange quarks. (Note that $\sum S_{hA}(j) = \sigma_{hA}$ where the sum extends over all stripping possibilities.)

The invariant cross section for inclusive production of hadrons in hadron-nucleus collisions $\sigma_A(h\to h') \equiv E[d^3\sigma_A(h\to h')/dp^3]$ at large x and small p_T can now be written as

$$\sigma_A(h\to h') = \sum_k \left[\frac{\sum_{j_k} S_{hA}(j_k)}{\sum_{j_k} S_{hN}(j_k)}\right] \sigma_N^k(h\to h')\,. \tag{6.5}$$

$\sigma_N^k(h\to h')$ is the contribution to the nucleon cross section from a quark diagram with a final hadron h' that contains the leading quark(s) k and the summation over j_k extends over all such diagrams. For production of h' that contains only a single leading quark, e.g., $p\to\pi,K,\ldots$ and $\pi\to\pi,K,\ldots$ or $\pi\to p,\Lambda,\ldots$, Eq. (6.5) leads, respectively, to

$$\sigma_A(p\to\pi,\ldots) = \frac{\sigma_{pA}-\sigma_{qA}}{\sigma_{pp}-\sigma_{qp}}\sigma_N(p\to\pi,\ldots)\,, \tag{6.6a}$$

$$\sigma_A(\pi\to K,\ldots) = \frac{\sigma_{\pi A}-\sigma_{qA}}{\sigma_{\pi p}-\sigma_{qp}}\sigma_N(\pi\to K,\ldots)\,. \tag{6.6b}$$

Similar relations can be derived for K initiated reactions. Note that Eqs. (6.6) predict an A dependence which does not change with x in agreement with the experimental measurements at large x ($x \gtrsim .5$) and small p_T.[29,30]

Production of baryons that can contain two leading quarks, such as $p\to n,\Lambda,\Sigma^0,\ldots$, can proceed via recombination of a single or two leading

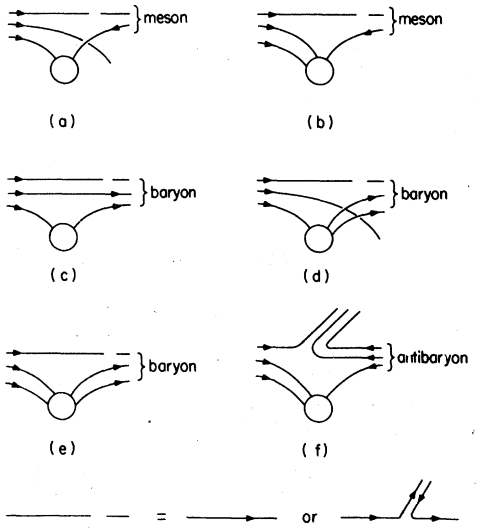

FIG. 9. Quark diagrams for production at large x and small p_T of mesons [(a), (b)] baryons [(c), (d), (e)], and antibaryons [(f)] by incident baryons.

quarks, as indicated in Figs. 9(c), 9(d), and 9(e), which give rise to two terms with different A and x dependences:

$$\sigma_A(p\to\Lambda,\dots)=\frac{\sigma_{pA}-\sigma_{\pi A}}{\sigma_{pp}-\sigma_{\pi p}}\sigma_N{}^2(p\to\Lambda,\dots)+\frac{\sigma_{pA}-\sigma_{qA}}{\sigma_{pp}-\sigma_{qp}}\sigma_N{}^1(p\to\Lambda,\dots). \quad (6.7)$$

Equation (6.7) can also be written as

$$\sigma_A(p\to\Lambda,\dots)=\frac{\sigma_{pA}-\sigma_{\pi A}}{\sigma_{pp}-\sigma_{\pi p}}\sigma_N(p\to\Lambda,\dots)+\frac{2\sigma_{\pi A}-\sigma_{pA}-\sigma_{qA}}{\sigma_{pp}-\sigma_{qp}}\sigma_N^1(p\to\Lambda,\dots). \quad (6.8)$$

The second term on the right-hand side of Eq. (6.7) increases with A faster than the first term. However, since the x distribution of a single valence quark is much steeper than that of a diquark, the relative importance of the second term increases when x decreases. This leads to a decreasing nuclear attenuation for smaller x values, in agreement with experiment.[29,30]

B. Recombination of wounded quarks

Next we show that the good agreement that was demonstrated in Ref. 34, between expressions (6.6), (6.8), and experimental measurements of production of hadrons with small p_T and large x, by both high-energy hadrons and leptons, is not destroyed by adding the contribution from the fragmentation and recombination of wounded quarks, i.e., of quarks that have suffered collisions within the nucleus.

Let us first consider production of particles that have only a single valence quark in common with the projectile, such as $pp\to\pi^\pm+X$. The produced particle can then be formed through a direct recombination of the valence quark from the projectile with a sea quark. If this valence quark has not lost momentum via collisions in the target, then the x distribution of the produced hadron is given by the x distribution of the valence quark in the projectile, i.e.,

$$\sigma_T(p\to M)=C_M^q(\sigma_{pT}-\sigma_{qT})q_p(x), \quad (6.9)$$

where $\sigma_T(p\to M)$ stands either for $E(d^3\sigma/dp^3)(pT\to M)$ at a fixed p_T or for its integral over p_T. C_M^q is a constant that depends on the specific recombination process, $q_p(x)$ is the x distribution of q in p, and T and M denote, respectively, the target particle and a meson.

Since only the quark-parton structure of nucleons is relatively well known (from deep-inelastic leptoproduction) we will limit our discussion to production of mesons by nucleons from nucleons, mesons, and nuclear targets. (Information on production from meson targets can be obtained by studying production in the backward c.m. hemisphere in meson-nucleon collisions.) To be more specific we will concentrate on π production by nucleons. Assuming isospin invariance and additive-quark-model relations among cross sections, we can write special cases of (6.9):

$$\begin{aligned}
&\sigma_N(p\to\pi^+)=\sigma_N(n\to\pi^-)=C_\pi^{u\,\frac{2}{3}}\sigma_{pp}u_p(x),\\
&\sigma_N(p\to\pi^-)=\sigma_N(n\to\pi^+)=C_\pi^{d\,\frac{2}{3}}\sigma_{pp}d_p(x),\\
&\sigma_M(p\to\pi^+)=\sigma_M(n\to\pi^-)=C_\pi^{u\,\frac{2}{3}}\sigma_{\pi p}u_p(x),\\
&\sigma_M(p\to\pi^-)=\sigma_M(n\to\pi^+)=C_\pi^{d\,\frac{2}{3}}\sigma_{\pi p}d_p(x),\\
&\sigma_A(p\to\pi^+)=\sigma_A(n\to\pi^-)=C_\pi^u(\sigma_{pA}-\sigma_{qA})u_p(x),\\
&\sigma_A(p\to\pi^-)=\sigma_A(n\to\pi^+)=C_\pi^d(\sigma_{pA}-\sigma_{qA})d_p(x).
\end{aligned} \quad (6.10)$$

The modifications of Eq. (6.10) due to recombination of wounded quarks can be estimated as follows: Since from each inelastic collision a wounded quark emerges with a new momentum distribution we therefore rewrite Eq. (6.9) in the form

$$\sigma_T(p\to M)=C_M^q\left[(\sigma_{pT}-\sigma_{qT})q_p(x)+\sigma_{qT}\sum_i P_q(i,T)q_p^{(i)}(x)\right]. \quad (6.11)$$

$P_q(i,A)$ is the probability that a quark q suffers i successive quark-nucleon collisions when it scatters from a nucleus A. It can be calculated using "standard nuclear optics techniques" as described in Sec. II. $P_q(i,A)$ for a few typical nuclei are tabulated in Appendix B.

$u_p^{(i)}(x)$ and $d_p^{(i)}(x)$ are the x distributions of the valence quarks of the incident proton after i successive quark-nucleon collisions. To estimate them we shall use gluon-photon analogy[38,39] (quark-lepton analogy), i.e., we will assume that the energy loss of a quark scattered from a nucleon (via a gluon exchange) is similar to the energy loss of a lepton scattered from a nucleon (via a photon or weak-vector-boson exchange). At present such an analogy can be justified on the basis of QCD only for deep-inelastic scattering. Moreover, we have also assumed that quarks neither fragment, nor recombine, nor change flavor between successive collisions. Such assumptions may be reasonable since formation times for small p_T particles are much longer than nuclear dimensions. In any case our assumptions tend to overestimate the contribution from recombinations of valence quarks that have suffered inelastic collisions which, as shown below, can be neglected at large values of x.

Let us denote by y the energy fraction lost by a

lepton in a deep-inelastic collision with a nucleon. Then the naive quark-parton model of the nucleon, which has exact Bjorken scaling behavior and satisfies the Callan-Gross relation leads to the following energy spectrum of the scattered lepton [see Eq. (3.6)]:

$$\frac{d\sigma}{dy}\sim 1-y+y^2/2 \tag{6.12a}$$

or

$$\frac{d\sigma}{dz}\sim z^2+1\,, \tag{6.12b}$$

where $z\equiv 1-y$ is the energy fraction retained by the lepton. The use of insight from deep-inelastic scattering to low-p_T processes is in the spirit of applying the parton model to both regions, although there is no justification for doing so in the second region. We use it here to investigate the effect of wounded quarks, which is anyhow found to be negligible. Thus the probability of a lepton or a quark to emerge from a deep-inelastic collision with a fraction z of its original energy is given by[39]

$$P_1(z)=\tfrac{3}{4}(z^2+1)\,. \tag{6.13}$$

The probability of a lepton or a quark to emerge from i deep-inelastic collisions with nucleons with a fraction z of its original energy is thus given by

$$P_i(z)=\int_z^1 P_1(z)P_{i-1}\left(\frac{z}{x}\right)\frac{dx}{x}\,, \tag{6.14}$$

and since $u_p(x)$ and $d_p(x)$ are the "original" momentum distributions of the valence quarks [as given for instance by Eqs. (2.6) and (2.7)],

$$u_p^{(i)}(x)=\int_x^1 u_p(x')P_i\left(\frac{x}{x'}\right)\frac{dx'}{x'} \tag{6.15a}$$

and

$$d_p^{(i)}(x)=\int_x^1 d_p(x')P_i\left(\frac{x}{x'}\right)\frac{dx'}{x'}\,. \tag{6.15b}$$

Except for very low values of x ($x\lesssim 0.03$), where our model is not applicable due to neglect of the contributions of sea quarks and gluons to particle production, the terms on the right-hand side of Eqs. (6.11) drop rapidly with i. We therefore consider here only the leading term and the term with $i=1$. [Approximate expressions for $P_i(z)$ and for $u_p^{(i)}(x)$ and $d_p^{(i)}(x)$ are given in Ref. 34.] For $i=1$ we obtain

$$u_p^{(1)}(x)=u_p(x)(1-x)^{\frac{3}{16}} \times\left[F(\tfrac{7}{2},1,5;1-x)+F(\tfrac{3}{2},1,5;1-x)\right] \tag{6.16a}$$

and

$$d_p^{(1)}(x)=d_p(x)(1-x)^{\frac{3}{20}} \times\left[F(\tfrac{7}{2},1,6;1-x)+F(\tfrac{3}{2},1,6;1-x)\right], \tag{6.16b}$$

which have the approximate behavior

$$u_p^{(1)}(x)\simeq\begin{cases}\dfrac{105}{256}(1-x)^4\,, & x\to 1\\[2ex] \dfrac{105}{64}\dfrac{(1-x)^3}{\sqrt{x}}\,, & x\to 0\end{cases} \tag{6.17a}$$

and

$$d_p^{(1)}(x)\simeq\begin{cases}\dfrac{189}{1024}(1-x)^5\,, & x\to 1\\[2ex] \dfrac{945}{1024}\dfrac{(1-x)^4}{\sqrt{x}}\,, & x\to 0.\end{cases} \tag{6.17b}$$

In Figs. 10 and 11 we compare predictions (6.10) and (6.11) with (6.16) and experimental results[40]

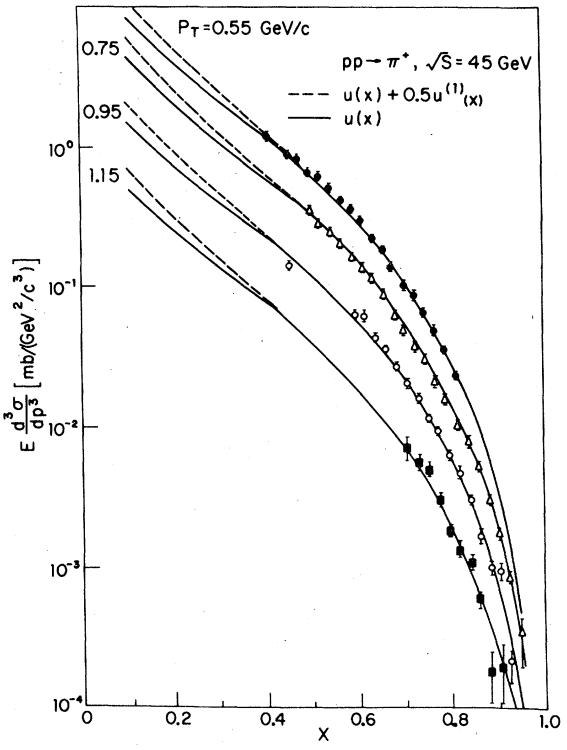

FIG. 10. Comparison between experimental results (Ref. 40) and our theoretical predictions for $E(d^3\sigma/dp^3)$ ($pp\to\pi^+$) at $p_T=0.55$, 0.75, 0.95, and 1.15 GeV/c as given by Eqs. (6.10) (dotted lines) and (6.11) (full lines) and as described in the text. The theoretical predictions were normalized to the experimental data. The dependence of the normalization constant on p_T (in GeV/c) is well described by $C_\pi^u\sim e^{-2.7p_T^2}$.

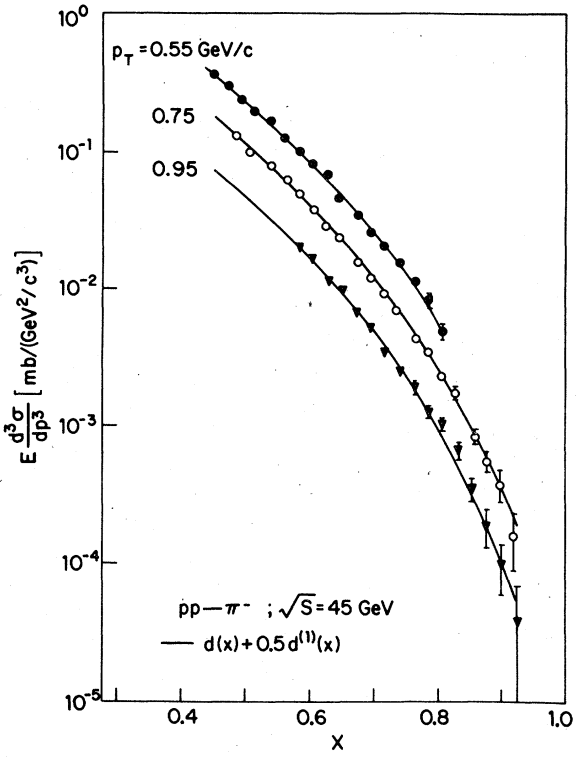

FIG. 11. Comparison between experimental results (Ref. 40) and our theoretical predictions for $E(d^3\sigma/dp^3) \times (pp \to \pi^-)$ at $p_T = 0.55$, 0.75, 0.95, and 1.15 GeV/c as given by Eq. (6.11) (full lines), and as described in the text. The theoretical predictions were normalized to the experimental data. The dependence of the normalization constant on p_T (in GeV/c) is well described by $C_\pi^d \sim e^{-2.7 p_T^2}$.

on $\pi^\pm$ production at large x and small p_T in pp collisions. As can be seen from Figs. 10 and 11, the contribution from wounded quarks is important only at small values of x and it does not destroy the good agreement between theory and experiment that has been demonstrated before[5] for large values of x.

The effect of wounded quarks on the A dependence of meson production at large x is demonstrated in Fig. 12. Since experimental results on production from nuclear targets are often parametrized as

$$R_{a\to b}(A_2/A_1) \equiv \sigma_{A_2}(a\to b)/\sigma_{A_1}(a\to b) \simeq (A_2/A_1)^{\alpha(x,p_T)}, \qquad (6.18)$$

in Fig. 12 we have compared our predictions for α and the experimental values for α that were obtained from measurements of $\pi^\pm, K^\pm$ production by 19 and 24 GeV/c protons[30(a),30(b)] and of K_S production by 300-GeV/c protons, from Be and

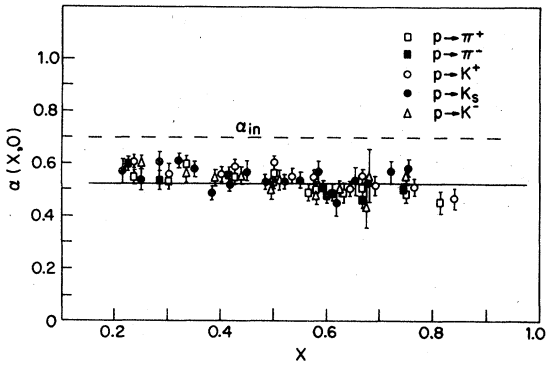

FIG. 12. Comparison between experimental measurements (Ref. 30) and quark-model predictions of $\alpha(x,0)$ as defined by Eq. (6.18) for meson production in high-energy p-A collisions. The line is our prediction for Pb/Be based on Eq. (6.16).

Pb targets.[30(d),30(e)] α for spectator quarks alone was calculated from Eq. (6.10) with the experimental proton-nucleus cross sections[41] and the values of σ_{qA} that are tabulated in Appendix B. α for spectator plus wounded quarks was calculated from Eqs. (6.11), (6.13)–(6.15), and the values of $P_q(i,A)$ that are tabulated in Appendix B; it is also shown in Fig. 12. As can be seen from Fig. 12 the inclusion of the contributions of wounded quarks does not affect α for large values of x and α is well described there by both Eqs. (6.10) and (6.11). At small values of x Eq. (6.11) deviates significantly from Eqs. (6.10) and it leads to an α which increases when x decreases, in good agreement with experiment. In Fig. 13 we present a comparison between experimental results[30(e)] and our theoretical predictions for $E(d^3\sigma/dp^3)(pA \to K_S^0(0°))$ at $p_{LAB} = 400$ GeV/c and A = Be, Cu, and Pb. Our predictions are based on Eqs. (6.11)–(6.15) and (2.7). σ_{pT} and σ_{qT} that were used are listed in Appendix B. To determine $C_{K_S^0}^d$ we used a best-fit procedure[42] from which we obtained the same value $C_{K_S^0}^d \cong 0.03$ (GeV^2/c^3)$^{-1}$ for Be, Cu, and Pb. Small deviations from a common constant can result from inaccurate values of σ_{pA} and/or σ_{qA}. In Fig. 14 we present the same comparison in terms of α as defined by Eq. (6.18).

The contribution of wounded quarks to production of baryons that contain two valence quarks in common with the projectile, such as $p \to \Lambda$, can also be estimated in a similar way: The produced baryon can be formed through a direct recombination of a valence quark or a diquark from the projectile with sea quarks. If the valence quark or diquark have not lost momentum via inelastic collisions in the target then the produced hadrons should have their x distribution in the projectile,

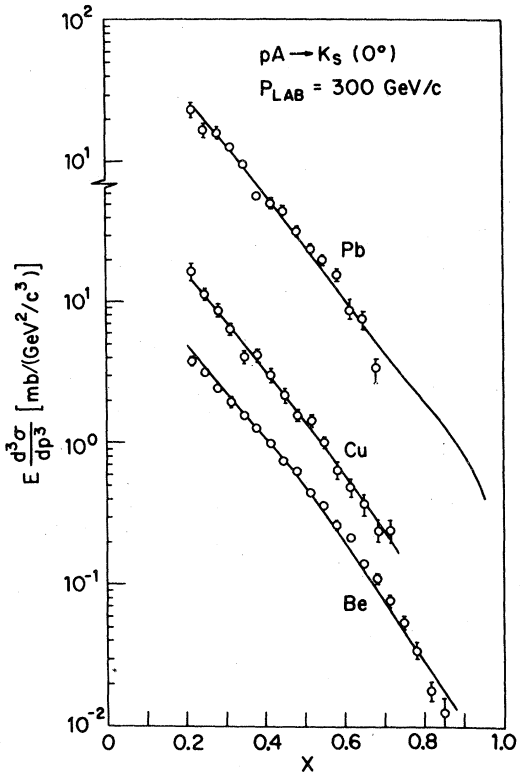

FIG. 13. Comparison between experimental results [Ref. 30(e)] and our theoretical predictions for $E(d^3\sigma/dp^3)(pA \to K_S^0(0°))$ at $p_{\mathrm{LAB}} = 300$ GeV/c and A = Be, Cu, and Pb. Details are given in the text.

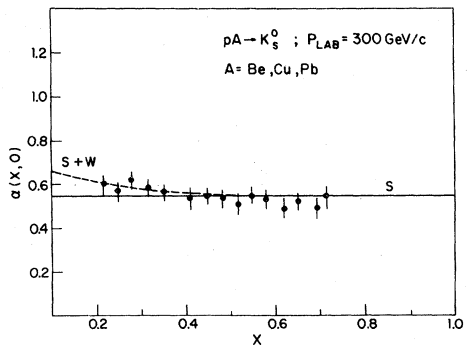

FIG. 14. Comparison between experimental results [Ref. 30(c)] on the A dependence of low-p_T K_S^0 production from nuclear targets (Be, Cu, Pb) by 300-GeV/c protons and the predictions of the quark recombination models. The full line represents the predictions for α when only spectator quarks recombine into K_S^0, as given by Eq. (6.10), while the dotted line represents the predictions for α when both spectator and wounded quarks recombine into K_S^0, as given by Eqs. (6.11).

i.e.,

$$\begin{aligned}\sigma_N(p\to\Lambda) &= C_\Lambda^D(\sigma_{pp}-\sigma_{\pi p})D_p(x)\\ &\quad+(\sigma_{pp}-\sigma_{qp})[C_p^u u_p(x)+C_p^d d_p(x)]\,,\\ \sigma_A(p\to\Lambda) &= C_\Lambda^D(\sigma_{pA}-\sigma_{\pi A})D_p(x)\\ &\quad+(\sigma_{pA}-\sigma_{qA})[C_p^u u_p(x)+C_p^d d_p(x)]\,.\end{aligned} \tag{6.19}$$

$D_p(x)$ is the x distribution of a diquark ud in a proton. C_Λ^D is its probability to recombine with an s quark from the sea to form Λ, and C_Λ^u and C_Λ^d are the probabilities, respectively, of a u quark and of a d quark from the proton to recombine with a diquark from the sea to form Λ. Longitudinal-phase-space counting rules (similar to those for nucleons in a tube) suggest that

$$D_p(x)\sim 6x(1-x)\,. \tag{6.20}$$

The contributions of wounded quarks can also be added to Eqs. (6.19). If one assumes that a deep-inelastic collision of a diquark breaks it, then only the contribution from single wounded quarks should be added to (6.19). However, the recombination probability of a single quark with a diquark from the sea may be very small and then the contribution from recombination of wounded diquarks may become important. If one assumes that the energy loss of a diquark in a collision with a nucleon is similar to that of a single quark one can write

$$\begin{aligned}\sigma_N(p\to\Lambda) &= \sigma_N^0(p\to\Lambda)+\sigma_{\pi p}C_\Lambda^D D_p(x)\\ &\quad+\sigma_{qp}[C_\Lambda^u u_p(x)+C_\Lambda^d d_p(x)]\,,\\ \sigma_A(p\to\Lambda) &= \sigma_A^0(p\to\Lambda)+\sigma_{\pi A}C_\Lambda^D\sum_{i=1}^{A}P_\pi(i,A)D_p^{(i)}(x)\\ &\quad+\sigma_{qA}\sum_{i=1}^{A}P_q(i,A)[C_\Lambda^u u_p^{(i)}(x)+C_\Lambda^d d_p^{(i)}(x)]\,,\end{aligned} \tag{6.21}$$

where the x distribution of a diquark after i inelastic collisions $D_p^{(i)}(x)$ is given by Eqs. (6.13)–(6.15) with u_p replaced by D_p. In particular

$$D_p^{(1)}(x)=\tfrac{9}{2}[x^2(2\ln x-1)+1]\,. \tag{6.22}$$

σ_N^0 and σ_Λ^0 are given by Eqs. (6.19).

In Fig. 15 we compare prediction (6.21) with experimental data[30(e)] on $pA\to\Lambda(0°)$ at p_{LAB} = 300 GeV and A = Be, Cu, and Pb. Since the sums on the right-hand side of (6.21) converge rapidly we have calculated only the first term of these sums. C_Λ^D, $C_\Lambda^u \cong C_\Lambda^d$ were determined by a best-fit procedure.[42] $C_\Lambda^D \cong 0.04$, $C_\Lambda^u \cong 0.01$ $(\mathrm{GeV}^2/c^3)^{-1}$. Figures 15 and 16 demonstrate that our model correctly predicts both the x dependence and the A dependence of Λ production from nuclei. (Figure 15 shows that within experimental errors C_Λ^D and $C_\Lambda^u \cong C_\Lambda^d$ are independent of A.)

In this section we have not tried to find a per-

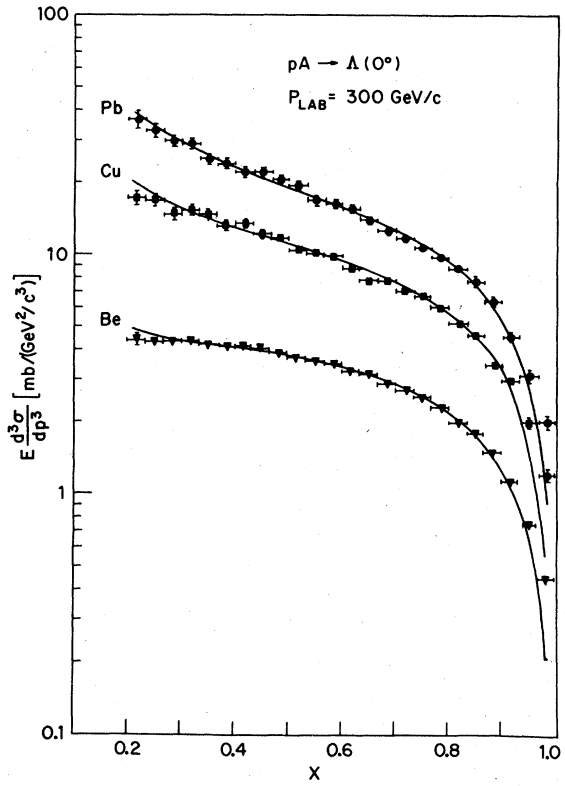

FIG. 15. Comparison between experimental results [Ref. 30(c)] and our theoretical predictions for $E(d^3\sigma/dp^3)(pA \to \Lambda(0°))$ at $p_{\mathrm{LAB}} = 300$ GeV/c and A = Be, Cu, and Pb. Details are given in the text.

fect agreement between theory and experiment (for instance, by improving the parametrization of quark distributions in nucleons and mesons and by including scaling-violating corrections). Our main purpose was to present some general mechanisms dominating large-x–low-p_T production upon which our explanation of cumulative production in Sec. VII is based, and to test them in some simple experimental situations. A more systematic investigation of large-x and low-p_T production is presented in Ref. 42.

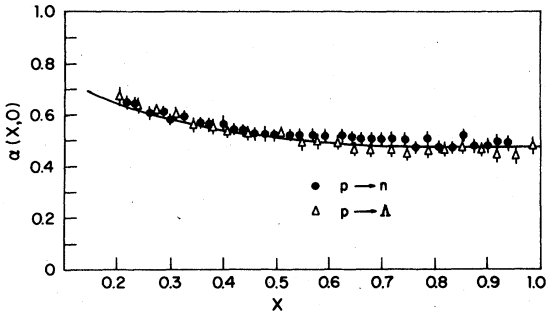

FIG. 16. Comparison between experimental results [Refs. 30(e) and 31] and theoretical predictions for $\alpha(x,0)$ of $E(d^3\sigma/dp^3)$ $(pA \to \Lambda)$ and $E(d^3\sigma/dp^3)$ $(pA \to n)$. Details are given in the text.

VII. CUMULATIVE PRODUCTION OF PARTICLES ON NUCLEI

The production of particles by high-energy projectiles incident on nuclei in kinematic regions not accessible in interactions with free stationary nucleons is possible due to the collective ("Fermi") motion of nucleons within nuclei. Such a phenomenon was first demonstrated by subthreshold production of antiprotons from nuclear targets.[25] Production of particles at backward angles with momenta exceeding those possible in interactions with a free stationary nucleon was first observed by Baldin and co-workers[43] who called it "cumulative production." Since then cumulative production at backward angles from nuclear targets has been extensively investigated at low, [44] medium,[45] and high energies.[46,47] Many theoretical models, for example, Refs. 48–54, have been applied to the data, but to the best of our judgement no model so far has offered a satisfactory explanation of the experimental data. In this section, however, we shall show that our quark-parton model of ultrarelativistic nuclei can explain remarkably well cumulative production at backward angles without the use of any free parameter.

When a high-energy projectile collides with a nucleus it interacts with all the nucleons that lie within a tube of cross section σ drawn along its straight path through the nucleus. Ignoring "friction forces," the rest of the nucleus is inactive during the collision and acts as a spectator. Ignoring also the cascading of reaction products inside the spectator part of the nucleus, we then can express a nondiffractive inelastic cross section of a nucleus as a sum of tube cross sections:

$$\sigma_A(a \to b) = \frac{\sigma^A}{\sigma} \sum_{i=1}^{A} P(i,A)\, \sigma_i(a \to b)\,. \tag{7.1}$$

σ^A/σ is the effective number of nuclear tubes, $P(i,A)$ is the probability that a tube contains exactly i nucleons, and $\sigma_i(a \to b)$ is the cross section for $a \to b$ on such a tube. Particles that are produced in the laboratory with large angles in the rest frame of the projectile a look like large-x particles that are produced by a high-energy tube incident on a. In particular,

$$\sigma_i(a \to b(180°)) = \sigma_a(i \to b(0°))\,. \tag{7.2}$$

Viewed in a high-momentum frame, such as the projectile rest frame, the valence quarks of the nucleons in a tube have the x distribution given by formulas (2.12) and (2.13). These valence quarks can produce hadrons with large x and small p_T via

direct recombination with sea quarks. The produced hadrons will have approximately the same x distribution as the valence quarks in the tube. Neglecting the contributions from wounded quarks we may write, for instance,

$$\sigma_p(i\to\pi^+)=C(\sigma_{pp}-\sigma_{qp})u_i(x) \tag{7.3a}$$

and

$$\sigma_p(i\to\pi^-)=C(\sigma_{pp}-\sigma_{qp})d_i(x)\,, \tag{7.3b}$$

where x is now the fraction of the *tube* c.m. momentum (in the projectile-tube c.m. frame) that is carried by the π, $C\simeq C_\pi^u\simeq C_\pi^d$ is a normalization constant, and u_i and d_i are given by (2.12) and (2.13), respectively. σ_{pp},σ_{qp} are pp,qp absorption cross sections, respectively.

Equations (7.3) have been written under the assumption that each quark in the tube penetrates through all the nucleons in front of it. If we take into account that a quark from a nucleon in a tube that recombines into the produced hadron must escape collisions with all the nucleons in front of it, including those in the projectile, while the diquark from the same nucleon must suffer at least one collision, we must rewrite Eqs. (7.3) as

$$\sigma_p(i\to\pi^+)=C\,\gamma(i)(\sigma_{pp}-\sigma_{qp})\,u_i(x) \tag{7.4a}$$

and

$$\sigma_p(i\to\pi^-)=C\,\gamma(i)(\sigma_{pp}-\sigma_{qp})\,d_i(x)\,, \tag{7.4b}$$

where

$$\gamma(i)=\frac{9}{14i}\left[6-7\left(\tfrac{2}{3}\right)^i+\left(\tfrac{2}{9}\right)^i\right]. \tag{7.5}$$

$\gamma(i)$ has been normalized such that $\gamma(1)=1$. It is derived in Appendix C under the assumption that the probability of a quark colliding when a proton hits another proton is $\sigma_{qp}/\sigma_{pp}=\frac{1}{3}$. We thus arrive at the result

$$\sigma_A(p\to\pi^+(180°))=\tfrac{2}{3}C\sigma_{pA}\sum_{i=1}^{A}P(i,A)\,\gamma(i)\,u_i(x) \tag{7.6a}$$

and

$$\sigma_A(p\to\pi^-(180°))=\tfrac{2}{3}C\sigma_{pA}\sum_{i=1}^{A}P(i,A)\,\gamma(i)\,d_i(x)\,. \tag{7.6b}$$

Moreover, if we assume factorization of the x distribution and the p_T distribution of the valence quarks within the nucleon, then since the Fermi momentum of nucleons within nuclei is approximately constant over the periodic table, we may also write for small P_T,

$$\sigma_A(p\to\pi^+)=f^{(+)}(p_T)\,\sigma_A(p\to\pi^+(180°))\,, \tag{7.7a}$$

$$\sigma_A(p\to\pi^-)=f^{(-)}(p_T)\sigma_A(p\to\pi^-(180°))\,. \tag{7.7b}$$

For pp collisions $f^{(+)}(p_T)$ and $f^{(-)}(p_T)$ can be well represented by[55]

$$f^{(\pm)}(p_T)=(e^{-10p_T^2}+0.45e^{-2.7p_T^2})/1.45\,. \tag{7.8}$$

In principle one should include in Eqs. (7.6) the contributions from wounded quarks, but since their calculations are very lengthy and tedious, and since they are rather small, we shall ignore them and we shall base our comparison between experiment and theory on Eqs. (7.6). However, before comparing Eqs. (7.6) with experiment, we would like to note that for medium and heavy weight nuclei our detailed numerical calculations show that over a wide range of x values the averaging over the different tubes can be well approximated by a single tube with ν_A nucleons, where $\nu_A\equiv A\sigma_{pp}/\sigma_{pA}$ is the average nuclear thickness. Thus

$$\sigma_A(p\to\pi^+(180°))\simeq\frac{\sigma_{pA}}{\sigma_{pp}}\sigma_{\nu_A}(p\to\pi^+(180°))$$
$$=\tfrac{2}{3}C\sigma_{pA}\,\gamma(\nu_A)u_{\nu_A}(x) \tag{7.9a}$$

and

$$\sigma_A(p\to\pi^-(180°))\simeq\frac{\sigma_{pA}}{\sigma_{pp}}\sigma_{\nu_A}(p\to\pi^-(180°))$$
$$=\tfrac{2}{3}C\sigma_{pA}\,\gamma(\nu_A)\,d_{\nu_A}(x). \tag{7.9b}$$

The deuteron is the simplest and the best understood nontrivial nucleus, so it is worth starting our comparison between experiment and theory by considering first backward production of pions from deuterium targets. With a Hulthén wave function for the deuteron Eq. (7.1) can be written as

$$\sigma_D(p\to\pi_b^\pm)=0.79\left[\sigma_p(p\to\pi_b^+)+\sigma_p(p\to\pi^-)\right]$$
$$+0.21\sigma_2(p\to\pi_b^\pm)\,. \tag{7.10}$$

We note, however, that for an aluminum target $\nu_A\simeq 2$ and with the aid of Eqs. (7.9) we obtain an approximate sum rule

$$\sigma_D(p\to\pi_b^\pm)=0.79\left[\sigma_p(p\to\pi_b^+)+\sigma_p(p\to\pi_b^-)\right]$$
$$+\,0.016\sigma_{Al}(p\to\pi_b^\pm)\,, \tag{7.11}$$

where π_b stands for π produced in the backward c.m. hemisphere. A similar sum rule can be written, of course, for π produced in the forward c.m. hemisphere (π_f)

$$\sigma_D(p\to\pi_f^\pm)=1.58\sigma_p(p\to\pi_f^\pm)$$
$$+\,0.016\sigma_{Al}(p\to\pi_f^\pm)\,. \tag{7.12}$$

Comparison between Eq. (7.11) and experiment provides a direct test of the tube hypothesis since Eq. (7.11) does not depend on the specific reaction mechanism for backward π production. The tube model combined with the quark-recombination model yields, however,

$$\sigma_D(p\to\pi_b^{\pm}) = 0.79\left[\sigma_p(p\to\pi_b^{+}) + \sigma_p(p\to\pi_b^{-})\right]$$
$$+0.21C_3^2\sigma_{pp}f(p_T)\left[\frac{21}{32}\frac{(1-x)^5}{\sqrt{x}}F(2.5,2,6;1-x) + \frac{63}{256}\frac{(1-x)^6}{\sqrt{x}}F(3.5,2,7;1-x)\right], \quad (7.13)$$

where $x \equiv p_L^*/p_{max}^*$, and p_L^* and p_{max}^* are, respectively, the longitudinal momentum of the π and the maximum momentum it can have in the pD c.m. system. For backward-produced pions by high-energy protons $x \simeq x_N/2$ where x_N is the corresponding variable in the pp c.m. system. In Fig. 17 we compare predictions (7.11) and (7.13) and the experimental results of Baldin *et al.*[45] on $pp \to \pi(180°)$ and pD$\to\pi(180°)$ at 8.6 GeV/c. To test predictions (7.11) we used Baldin's data[43] on pAl$\to\pi(180°)$ at $p_{LAB} = 8.4$ GeV/c. To test prediction (7.13) we have first used Baldin's data[45] on $pp \to \pi(180°)$ at 8.6 GeV/c to find $C_\pi^u \simeq C_d^u$ and with these values we then calculated the right-hand side of (7.13). As can be seen both predictions (7.11) and (7.13) are in remarkable agreement with experiment.

Expression (7.13) has also been tested recently by Hanlon *et al.*[56] in pD collisions at 100 and 400 GeV/c and in πD collisions at 100 GeV/c. These authors first tested Eq. (6.10b) against their data on fragmentation of neutrons at 100 and 400 GeV/c on a proton and at 100 GeV/c on a pion. Their comparison is presented in Fig. 18. As can be

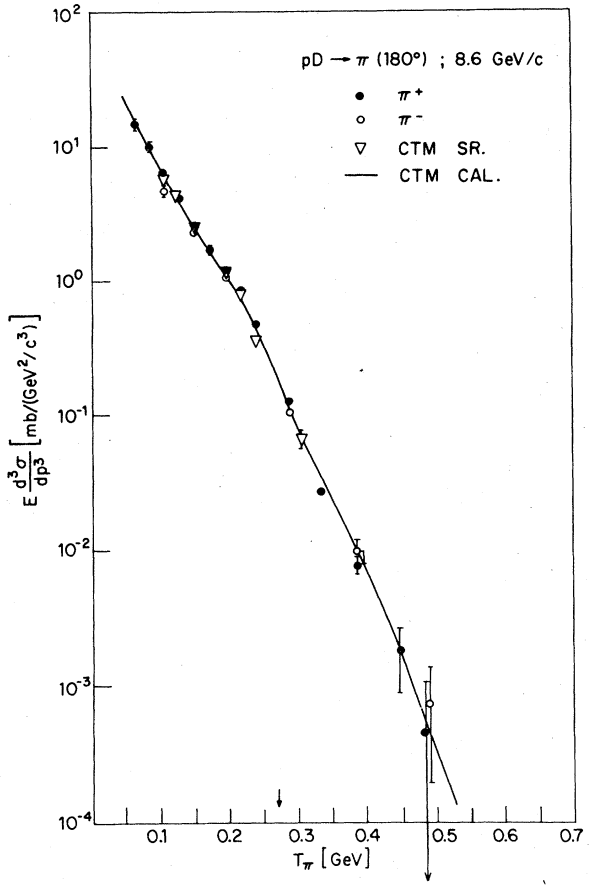

FIG. 17. Comparison between the collective-tube-model (CTM) sum rule (7.11) (triangles), the theoretical prediction (7.13) (full line) and experimental results (Ref. 49) on $E(d^3\sigma/dp^3)$ (pD$\to\pi^{\pm}(180°)$) as function of $T_\pi = E_\pi - m_\pi$ at $p_{lab} = 8.6$ GeV/c. The CTM sum rule was evaluated from experimental data on $pp \to \pi^{\pm}(0°)$ at $p_{lab} = 8.6$ GeV/c (Ref. 45) and on pAl$\to\pi^{\pm}$ (180°) at $p_{LAB} = 8.4$ GeV/c (Ref. 43). Arrows indicate T_π (max) for production on a single stationary nucleon.

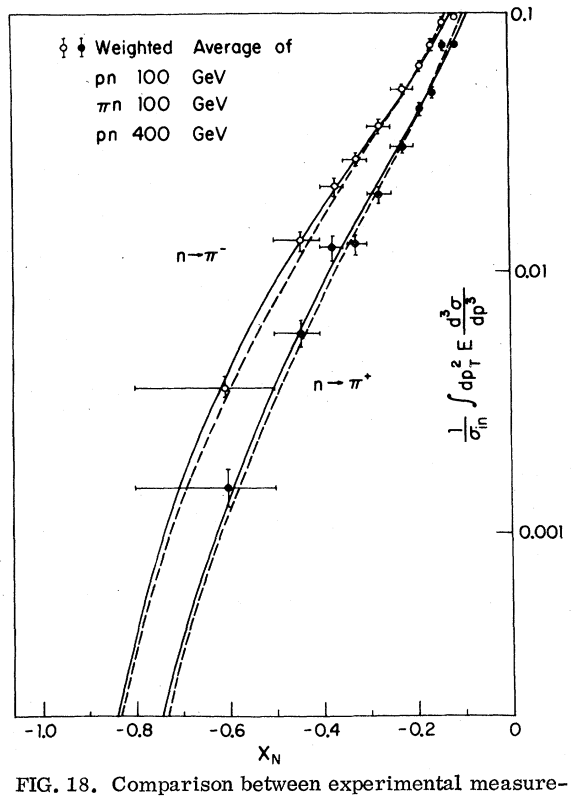

FIG. 18. Comparison between experimental measurements (Ref. 56) of inclusive production of $\pi^{\pm}$ by neutrons as extracted from 100-GeV pD and πD collisions and 400-GeV pD collisions, and the predictions of the quark-recombination models. The full lines represent the cross sections due to recombination of spectator quarks as given by Eqs. (6.10) with $C_\pi^u = 0.32$ and $C_\pi^d = 0.47$ (obtained by a best-fit procedure), while the dotted lines represent the cross sections due to recombination of both spectator and wounded quarks as given by Eqs. (6.11) with $C_\pi^u = 0.25$ and $C_\pi^d = 0.39$ (obtained by best-fit procedure). The experimental points are the weighted average of the three experiments.

seen from this figure agreement between experiment and theory is very good. They obtained $C_\pi^u \cong 0.32$ $(\mathrm{GeV}^3/c^2)^{-1}$ and $C_\pi^d \cong 0.47$ $(\mathrm{GeV}^2/c^3)^{-1}$. With these values they calculated expression (7.13) and compared it with their data on backward π production in pD and πD collisions. Their comparison is presented in Fig. 19. As can be seen, agreement between experiment and theory is good, except at small values of $|x|$ where (7.13) is not expected to correctly describe the experimental data. In Figs. 20–24 we compare expressions (7.6) and experimental data[45] on $p\mathrm{He} \to \pi(180°)$ at $p_{\mathrm{LAB}} = 8.6$ GeV/c and on $pA \to \pi^\pm(180°)$ at $p_{\mathrm{lab}} = 6$ and 8.4 GeV/c where $A = {}^{12}$C, Al, Cu, and Pb.[43] In Fig. 25 we compare the dependence of $\sigma(p\mathrm{Pb} \to \pi^+)$ on θ_{LAB} as predicted by expressions (7.6) and (7.7), and experimental data[45] at $p_{\mathrm{LAB}} = 8.6$ GeV/c for a fixed pion momentum $p_\pi = 0.5$ GeV/c. From Figs. 17–25 we conclude that the A dependence, the x dependence, and the θ dependence of $\pi^\pm$ produced backward in the laboratory in pA collisions, at incident energy $p_{\mathrm{LAB}} \simeq 8.5$ GeV/c, are well described by our model. It is important to note that the comparison between theory and experiment extends to pion kinetic energies which cannot be obtained if the production took place on individual stationary nucleons. If we denote by $T_\pi = E_\pi - m_\pi$ the kinetic energy of a pion produced backward in the laboratory, then for $p_{\mathrm{LAB}} = 8.4$ GeV/c, $T_\pi(\mathrm{max}) = 0.27$, 0.62, 0.94, 1.23 GeV for targets of a mass of, respectively, one, two, three, four nucleons. We also note that while expressions (6.10) with (2.6) and (2.7) well describe $\pi^\pm$ production in pp collisions at high energies ($p_{\mathrm{LAB}} \gtrsim 100$ GeV/c) they do not describe so well $\pi^\pm$ production in pp collisions at few GeV. (It is possible that this violation of Feynman scaling is related to violations of Bjorken scaling.) If one would like to apply our model to backward $\pi^\pm$ production in pA collisions at such low energies one should substitute in Eq. (2.2) quark distribution functions that well describe $\pi^\pm$ production in pp collisions at such low energies, and use the resulting quark distributions in nuclear tubes instead of (2.12) and (2.13).

$\pi^\pm$ production from nuclear targets at backward angles by 400-GeV/c protons has been studied recently at Fermilab. Preliminary results were published[47] on pTa collisions. In Fig. 26 we present a comparison between the experimental re-

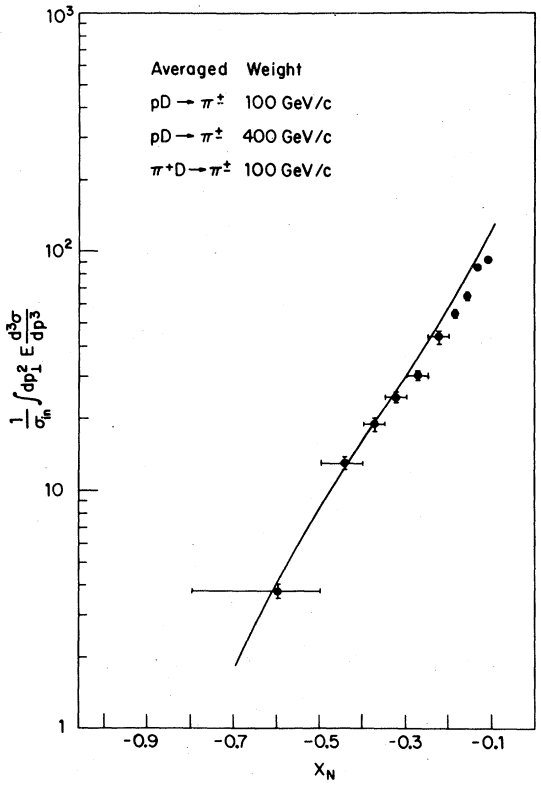

FIG. 19. Comparison between the theoretical prediction (7.13) and experimental results (Ref. 56) on $E(d^3\sigma/dp^3)$ $(p\mathrm{D} \to \pi_b^\pm)$ at $p_{\mathrm{LAB}} = 100$ and 400 GeV/c and on $E(d^3\sigma/dp^3)$ $(\pi\mathrm{D} \to \pi_b^\pm)$ at 100 GeV/c. The experimental points are the weighted average of the three experiments.

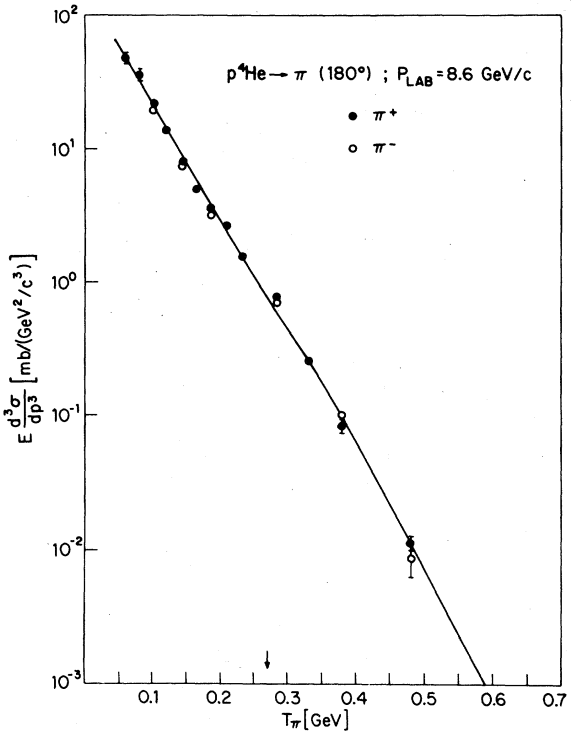

FIG. 20. Comparison between the theoretical predictions (7.6) and experimental results (Ref. 45) on $E(d^3\sigma/dp^3)$ $(p\,{}^4\mathrm{He} \to \pi^\pm(180°))$ as function of $T_\pi = E_\pi - m_\pi$ at $p_{\mathrm{LAB}} = 8.6$ GeV/c.

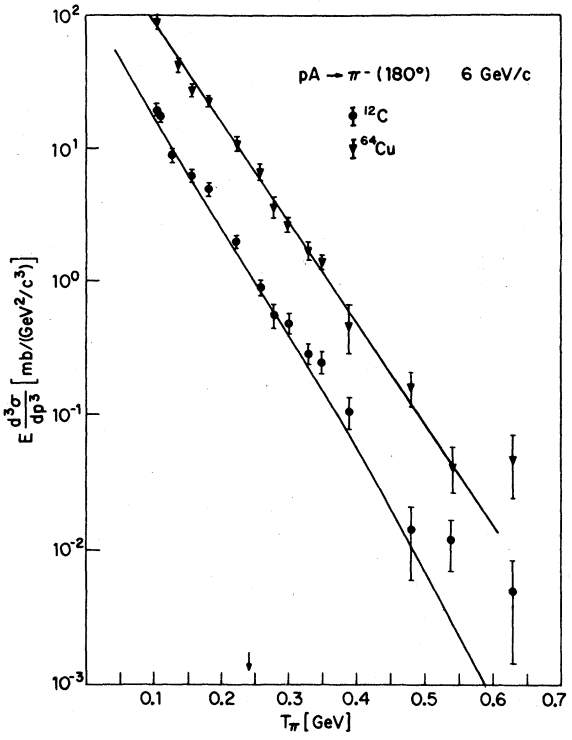

FIG. 21. Comparison between the theoretical predictions (7.6b) and experimental results (Ref. 43) on $E(d^3\sigma/dp^3)$ $(pA \to \pi^-(180°))$ as function of $T_\pi = E_\pi - m_\pi$ at $p_{\mathrm{LAB}} = 6$ GeV/c for $A = {}^{12}$C and ^{64}Cu.

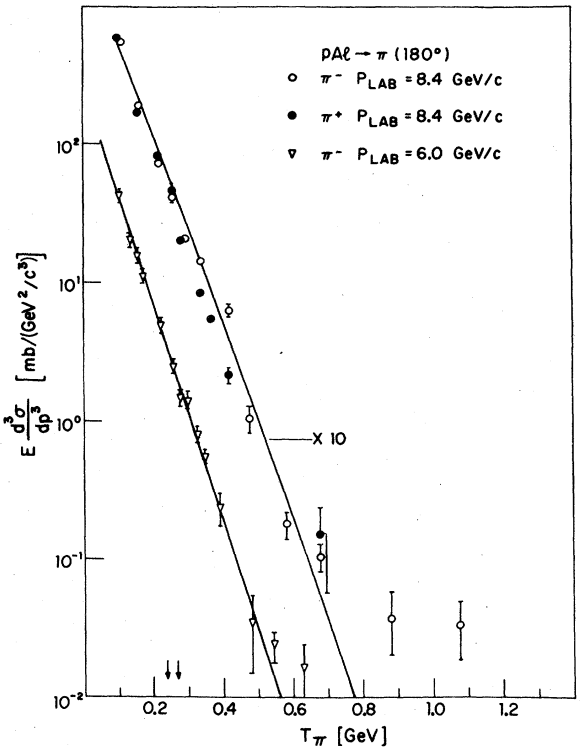

FIG. 22. Comparison between the theoretical predictions (7.6a) and experimental results (Ref. 43) on $E(d^3\sigma/dp^3)$ $(pAl \to \pi^\pm(180°))$ as function of $T_\pi = E_\pi - m_\pi$ at $p_{\mathrm{LAB}} = 6.0$ and 8.4 GeV/c.

sults on $E(d^3\sigma/dp^3)(p\mathrm{Ta} \to \pi^\pm(180°))$ as function of T_π and predictions (7.6) and (7.9). With the values of $C_\pi^u \cong C_\pi^d \cong 0.4$ (GeV/c)$^{-1}$ that was obtained from $pp \to \pi^\pm$ at the same energy. As can be seen from Fig. 26, both the exact predictions (7.6) and the approximate prediction (7.9) well describe the experimental results. In Fig. 27 we compare the experimental results[47] on the A dependence of $E(d^3\sigma/dp^3)(pA \to \pi^\pm)$ for $p_\pi = 0.68$ GeV/c at $p_{\mathrm{LAB}} = 400$ GeV/c and at fixed laboratory angles $\theta_{\mathrm{LAB}} = 90°, 135°$, and 180°, and our theoretical predictions as given by expressions (7.6) and (7.7). As can be seen from Fig. 27 agreement between theory and experiment is very good. Finally in Fig. 28 we compare experimental data on the pion spectrum $\int_{T_\pi}^{0.428} E(d^3\sigma/dp^3)dT_\pi$ at $\theta_{\mathrm{LAB}} = 180°$ produced by protons incident on Ta, at $p_{\mathrm{LAB}} = 8.4$ GeV/c (interpolated data[43]), 28.5 GeV/c (Ref. 46), and 400 GeV/c (Ref. 48), and the spectrum predicted from expressions (7.6). Also, Fig. 28 demonstrates good agreement between experiment and theory.

The success of our model in predicting correctly all the features of inclusive production of $\pi^\pm$ at backward laboratory angles in high-energy pA collisions, i.e., the x dependence, the A dependence, and the θ_{LAB} dependence of $E(d^3\sigma/dp^3) \times (pA \to \pi^\pm)$ in kinematical domains which are not accessible to production from a single stationary nucleon, is the strongest support so far for the validity of our quark-parton model of a nucleus in a high-momentum frame.

Our model can be further improved by using better parametrizations than (2.6) and (2.7) for u_p and d_p, respectively, by introducing QCD scaling-violating corrections, especially in u_p and d_p and by including the contribution from wounded quarks. Both such improvements and the generalization of our model to backward production of other fragments, such as $K^\pm, K^0, \Lambda, \mathrm{D}, {}^3$He, etc., will be considered in a forthcoming publication.

VIII. SUMMARY AND CONCLUSIONS

In this article we have presented a quark-parton model for interactions with nuclei. This model, based on the tube picture, replaces our previous universality assumption (independence on in-

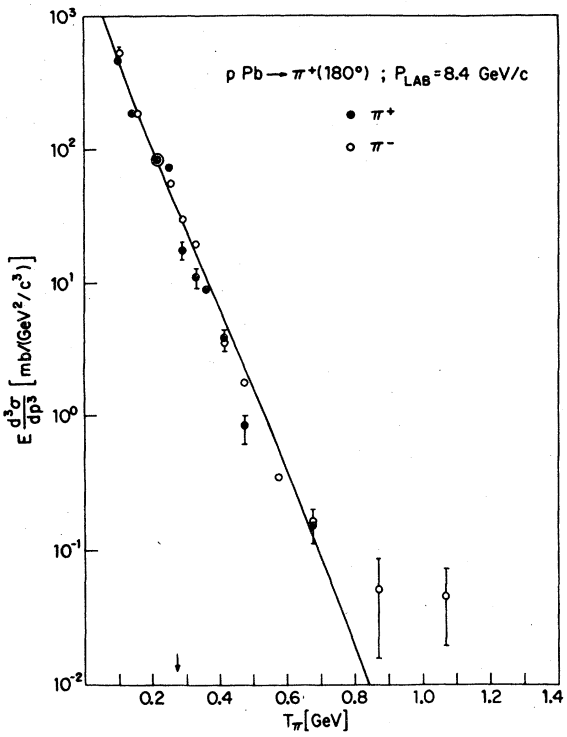

FIG. 23. Comparison between the theoretical prediction (7.6a) and experimental results (Ref. 45) on $E(d^3\sigma/dp^3)$ $(p\,\mathrm{Pb}\to\pi^{\pm}(180°))$ as function of $T_\pi = E_\pi - m_\pi$ at $p_{\mathrm{LAB}} = 8.4$ GeV/c.

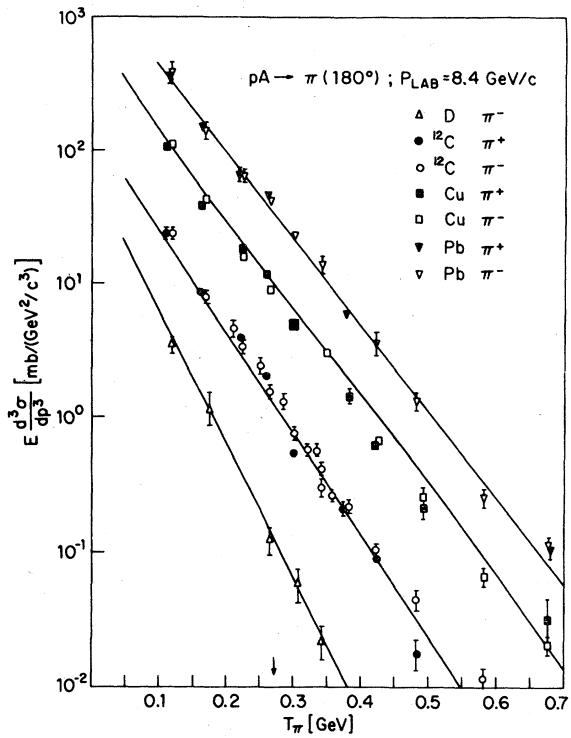

FIG. 24. Comparison between the theoretical predictions (7.6a) and (7.13) and experimental results (Ref. 43) on $E(d^3\sigma/dp^3)$ $(pA\to\pi^{\pm}(180°))$ as function of $T_\pi = E_\pi - m_\pi$, at $p_{\mathrm{LAB}} = 8.4$ GeV/c for A = D, C, Cu, and Pb.

coming quantum numbers) and the assumption that u quark distributions in a tube behave as $(1-x_{qt})^{6i-3}$ with a more reasonable and phenomenologically satisfactory hierarchial picture of quarks in nucleons, nucleons in tubes, and tubes in nuclei.

Is there a crucual test for the picture presented here? Backward scattering off nuclei is such a test. Although for a specific nucleus one can explain the data with an abnormal *ad hoc* Fermi motion, the A dependence remains a puzzle for Fermi-motion models. The features of the backward data are reproduced here for the first time over a wide range of incoming energies, targets, projectiles, outgoing particles, and outgoing angles and momenta.

Other important tests are the following: (1) Subthreshold production of heavy particles and its A dependence. We plan to present such predictions (other than for W bosons which is included here) and the A dependence of jet production (α_{exp} may reach 1.8) in a future publication. (2) Deep-inelastic production for high x and for various nuclei. (3) For μ pairs $\alpha > 1$ for large Q^2 is a unique prediction of our model, as well as the prediction $\alpha_p > \alpha_\pi$ (p and π are the projectiles).

ACKNOWLEDGMENT

This work was supported in part by the U. S.-Israel Binational Science Foundation, and by the Israel Commission for Basic Research.

APPENDIX A

Consider the phase space of i identical particles of mass m, uncorrelated except for energy con-

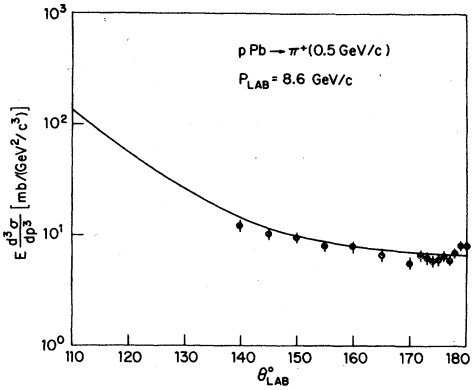

FIG. 25. Comparison between the theoretical predictions (7.6a) and (7.7a) and experimental results (Ref. 45) on $E(d^3\sigma/dp^3)$ $(p\,\mathrm{Pb}\to\pi^{+})$ at backward angles as function of $\Theta_{\mathrm{LAB}} = 8.6$ GeV/c.

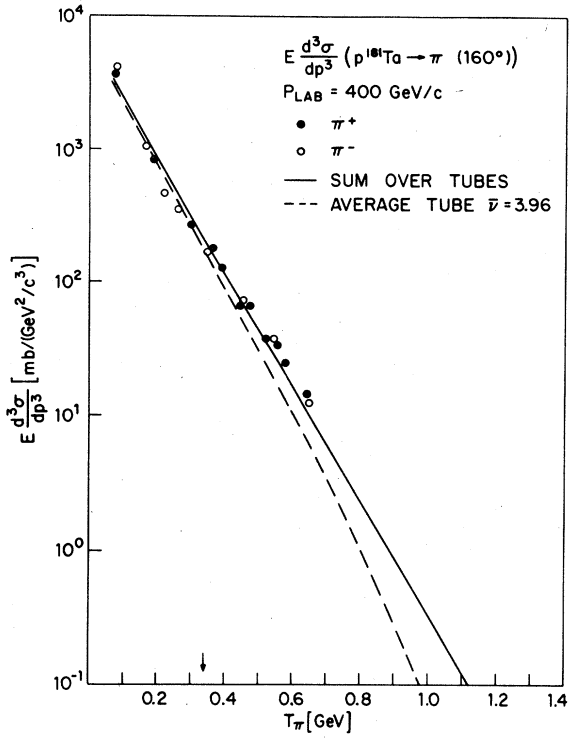

FIG. 26. Comparison between the theoretical predictions (7.6a) and (7.7a) (full line), the approximate prediction (7.9a) with $\bar{\nu}=3.96$ (dotted line) and experimental results (Ref. 47) on $E(d^3\sigma/dp^3)$ (p ^{181}Ta $\rightarrow \pi^{\pm}$) at $\Theta_{LAB}=160°$ as function of $T_\pi = E_\pi - m_\pi$ at $p_{LAB}=400$ GeV/c.

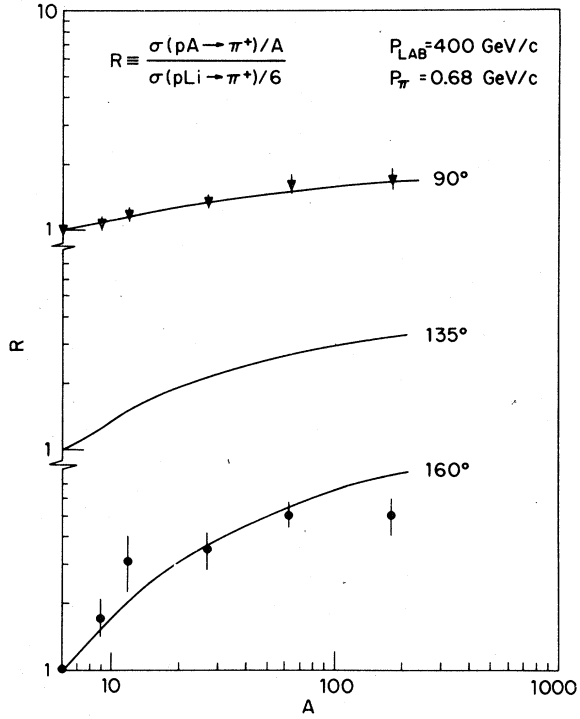

FIG. 27. Comparison between the theoretical predictions (7.6a) with p_T dependence as given by (7.8) and experimental results (Ref. 47) on the ratio $A^{-1}E(d^3\sigma/dp^3)$ ($pA \rightarrow \pi^+)/6^{-1}E(d^3\sigma/dp^3)$ (p ^{6}Li $\rightarrow \pi^+$) at $p_\pi = 0.68$ GeV/c and $p_{LAB}=400$ GeV/c as function of A, for $\Theta_{LAB}=90°$, 135°, and 160°.

servation:

$$P_i(E) = \int \prod_{j=1}^{i} \frac{d^3p_j}{2E_j}\,\delta\left(E - \sum_{k=1}^{i} E_k\right) = \int \delta\left(E - \sum_{k=1}^{i} E_k\right) \prod_{j=1}^{i} \delta(p_j^2 - m^2)\theta(p_j)\,d^4p_j . \tag{A1}$$

Its Laplace transform $L_i(\alpha)$ is defined through

$$L_i(\alpha) = \int e^{-\alpha E} P_i(E)\,dE . \tag{A2}$$

Substituting (A1) into (A2) yields

$$L_i(\alpha) = [l(\alpha)]^i , \tag{A3}$$

where

$$l(\alpha) = \int e^{-\alpha p_0}\,\delta(p^2 - m^2)\theta(p)\,d^4p = \frac{2\pi m}{\alpha} K_1(\alpha m) . \tag{A4}$$

K_1 is the modified Bessel function which has the integral representation

$$K_1(x) = x\int_1^\infty e^{-xy}(y^2-1)^{1/2}\,dy .$$

In the limit $\alpha \rightarrow 0$, $l(\alpha) \rightarrow 2\pi/\alpha^2$ and

$$L_i(\alpha) \sim \left(\frac{2\pi}{\alpha^2}\right)^i . \tag{A5}$$

In this limit (A2) is dominated by contribution from large values of E. By equating (A2) and (A5) we find that for large E

$$P_i(E) \simeq \frac{(2\pi)^i}{(2i-1)!} E^{2i-1} . \tag{A6}$$

If particle j carries a fraction x of the total energy (longitudinal momentum) then the phase space of the $i-1$ spectators, according to (A6), is

$$P_{i-1}[(1-x)E] = \frac{(2\pi)^{i-1}}{(2i-3)!} E^{2i-3}(1-x)^{2i-3} , \tag{A7}$$

while the phase-space density of the particle j is $p_j dp_j \sim E^2 x\,dx$. Since particle j can be any one of the i particles, therefore, the relative phase space to find a particle with a fraction x of the total energy is

$$N_i(x)dx = \frac{iE^2x\,dx P_{i-1}[(1-x)E]}{P_i(E)} = i(2i-2)(2i-1)\,x(1-x)^{2i-3} . \tag{A8}$$

TABLE I. $P(i,A)$ as calculated from Eqs. (2.19)–(2.22) with $\sigma_{qp}^{t}=33$ mb and a Woods-Saxon nuclear density function.

		$P(i,A)$ in %										σ_{pA} (mb)	
A	i	1	2	3	4	5	6	7	8	9	10	Theor.	Expt. (± 5%)
^{4}He		79.95	17.31	2.56	0.17							129	
^{6}Li		73.08	21.02	5.02	0.80	0.07						175	174
^{9}Be		65.90	23.75	7.90	2.01	0.37	0.05					224	210
^{12}C		60.74	25.00	10.01	3.24	0.82	0.16	0.02				274	248
^{27}Al		46.69	25.28	14.90	7.78	3.46	1.31	0.42	0.12	0.03		474	445
^{64}Cu		33.87	21.49	16.41	11.93	7.79	4.50	2.31	1.05	0.43	0.16	824	796
^{119}Sn		26.52	17.58	14.97	12.81	10.20	7.38	4.83	2.85	1.53	0.75	1215	1259
^{207}Pb		21.30	14.15	12.65	11.92	10.83	9.19	7.17	5.13	3.37	2.04	1711	1812

TABLE II. $P_q(i,A)$ as calculated from Eqs. (2.19)–(2.22) with $\sigma_{qp}^{t}=13$ mb and a Woods-Saxon nuclear density function.

		$P_q(i,A)$ in %										
A	i	1	2	3	4	5	6	7	8	9	10	σ_{qA} (mb)
^{4}He		91.81	7.78	0.41	0.01							47.0
^{6}Li		88.35	10.64	0.95	0.05							69.2
^{9}Be		84.33	13.70	1.79	0.17	0.01						99.3
^{12}C		81.15	15.91	2.59	0.32	0.03						127.7
^{27}Al		70.92	21.73	5.82	1.26	0.22	0.03					253.9
^{64}Cu		58.59	26.14	10.50	3.50	0.98	0.23	0.05				510.2
^{119}Sn		49.38	27.44	14.02	6.02	2.19	0.69	0.19	0.05			825.9
^{207}Pb		41.31	27.04	16.68	8.80	3.93	1.53	0.52	0.16	0.04	0.01	1253.0

TABLE III. $P_\pi(i,A)$ as calculated from Eqs. (2.19)–(2.22) with $\sigma_{\pi p}^{t}=26$ mb and a Woods-Saxon nuclear density function.

		$P_\pi(i,A)$ in %										$\sigma_{\pi A}$ (mb)	
A	i	1	2	3	4	5	6	7	8	9	10	Theor.	Expt. (± 5%)
^{4}He		83.98	14.33	1.61	0.08							88.3	
^{6}Li		78.04	18.16	3.36	0.41	0.03						123.6	123
^{9}Be		71.60	21.47	5.64	1.11	0.16	0.02					171.0	152
^{12}C		66.81	23.36	7.50	1.90	0.37	0.05					214.9	181
^{27}Al		53.02	26.04	12.85	5.42	1.91	0.57	0.14	0.03			390.8	342
^{64}Cu		39.31	24.41	16.58	10.16	5.43	2.52	1.03	0.37	0.12	0.03	715.5	647
^{119}Sn		30.89	21.14	16.90	12.68	8.51	5.06	2.68	1.27	0.54	0.21	1086	1045
^{207}Pb		24.63	17.58	15.52	13.42	10.64	7.62	4.91	2.87	1.52	0.74	1566	1548

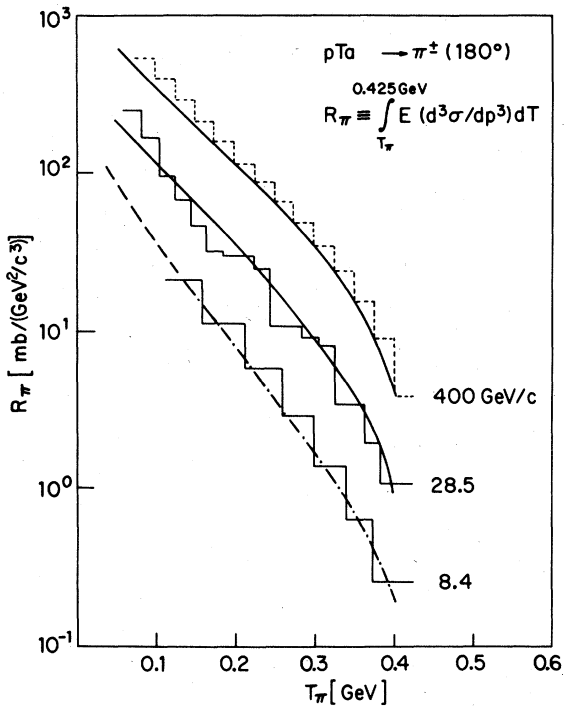

FIG. 28. Comparison between the theoretical predictions based on (7.6) and experimental results on the energy dependence of the $\pi^\pm$ spectrum $\int_T^{0.425\,\mathrm{GeV}} E(d^3\sigma/dp^3)\,(p\,^{181}\mathrm{Ta}\to\pi^\pm(180°))\,dT_\pi$. The "experimental data" at 8.4 GeV/c was obtained by interpolating the data of Ref. 43. The experimental data at 28.5 GeV/c is from Ref. 46 and at 400 GeV/c is from Ref. 47.

APPENDIX B

In Tables I, II and III we present the results of our calculations of $P(i,A)$ for $\sigma=\sigma^{t}_{qp}$, $\sigma^{t}_{\pi p}$, and σ^{in}_{pp}, respectively. The numerical calculations are based on Eqs. (2.19)–(2.22) and they use a standard Woods-Saxon nuclear density function

$$\rho(r)=\rho_0\{1+\exp[(R-r)/d]\}^{-1}$$

with

$$R=1.10\ A^{1/3}\ \mathrm{fm},\quad d=0.54\ \mathrm{fm}.$$

This choice of $\rho(r)$ well reproduces the experimental values[41] of the nuclear absorption cross sections of p and π when $\sigma^{t}_{pp}=39$ mb and $\sigma^{t}_{\pi p}=26$ mb are used in

$$\sigma_{pA}=\int\left\{1-\left[1-\frac{\sigma T(b)}{A}\right]^{A}\right\}d^2b\,.$$

APPENDIX C

We shall derive here the relative probability of a quark in a tube recombining into a large-x–low-p_T hadron when a tube fragments on a target proton, compared to that of a quark in a single nucleon which fragments on a target proton.

According to the additive quark model the probability of a quark in a nucleon escaping collision when the nucleon collides with a target proton is $1-\sigma_{qp}/\sigma_{pp}=\frac{2}{3}$. If there are j nucleons in front of it, its probability of penetrating them without collision is $(\frac{2}{3})^j$ while the probability that the nucleon will actually fragment, i.e., that the remaining diquark suffers a collision is $1-(1-\frac{2}{3})^j$. The joint probability is therefore $(\frac{2}{3})^j[1-(\frac{1}{3})^j]$ and the relative probability is $(\frac{2}{3})^j[1-(\frac{1}{3})^j]/\frac{4}{9}$. If we average this probability over all nucleons in a tube of i nucleons we obtain

$$\gamma(i)=\frac{9}{14i}\sum_{j=1}^{i}(\tfrac{2}{3})^j[1-(\tfrac{1}{3})^j]$$

$$=\frac{9}{14i}[6-7(\tfrac{2}{3})^i+(\tfrac{2}{9})^i]\,. \qquad \text{(C1)}$$

Above we have assumed that one quark passes through the tube unaffected, while a diquark system interacts with the tube nucleons as a single object. An alternative way to derive the attenuation factor is to assume that the two quarks interact with the tube nucleons independently, and then the attenuation is $(\frac{2}{3})^j[1-(\frac{2}{3})^{2j}]$.

After averaging over i and normalizing the attenuation factor such that for a tube with a single nucleon $\gamma'(i)=1$, we obtain

$$\gamma'(i)=\frac{81}{19i}\left[1-\frac{19}{15}\left(\frac{2}{3}\right)^i+\frac{4}{15}\left(\frac{8}{27}\right)^i\right]. \qquad \text{(C2)}$$

$\gamma(i)$ and $\gamma'(i)$ are compared in Table IV. As can be seen from Table IV $\gamma(i)$ and $\gamma'(i)$ are numerically very similar. In the present work we used $\gamma(i)$ as the attenuation factor. The use of $\gamma'(i)$ instead does not lead to any noticeable changes in our numerical results and comparisons with experiments.

TABLE IV. Comparison between $\gamma(i)$ and $\gamma'(i)$ as a function of i as given, respectively, by expressions (C1) and (C2).

i	$\gamma(i)$	$\gamma'(i)$
1	1.000	1.000
2	0.944	0.981
3	0.844	0.898
4	0.742	0.801
5	0.653	0.711
6	0.577	0.632
7	0.513	0.553
8	0.460	0.506
9	0.415	0.458
10	0.378	0.417

[1]For a recent review of high-energy particle-nucleus collisions see, for instance, L. Bergstrom, S. Fredriksson, G. Berlad, and G. Eilam, Phys. Rep. (to be published).

[2]R. P. Feynman, Phys. Rev. Lett. 23, 1415 (1969); R. P. Feynman, *Photon-Hadron Interactions* (Benjamin, Reading, Mass., 1972); J. D. Bjorken and E. A. Paschos, Phys. Rev. 185, 1975 (1969); J. Kuti and V. F. Weisskopf, *ibid.* 185, 1975 (1969). For a recent review see, for instance, P. Roy, *Theory of Lepton-Hadron Processes at High Energies* (Clarendon, Oxford, 1975).

[3]For reviews on QCD see, for instance, H. D. Politzer, Phys. Rep. 14C, 129 (1974); W. Marciano and H. Pagels, *ibid.* 36C, 137 (1978); V. A. Novikov *et al.*, *ibid.* 41C, 1 (1978); A. J. Buras, Rev. Mod. Phys. 52, 199 (1980).

[4]J. D. Bjorken, Phys. Rev. 179, 1547 (1969).

[5]For quark recombination models see, for instance, H. Goldberg, Nucl. Phys. B44, 149 (1972); S. Pokorski and L. Van Hove, Acta Phys. Pol. B5, 229 (1974); Nucl. Phys. B86, 243 (1975), CERN Report No. TH.9427, 1977 (unpublished); L. Van Hove, Acta Phys. Pol. B7, 339 (1976); Acta Phys. Austriaca Suppl. 21, 621 (1979); W. Ochs, Nucl. Phys. B118, 397 (1977); K. P. Das and R. C. Hwa, Phys. Lett. 68B, 459 (1977); D. W. Duke and F. E. Taylor, Phys. Rev. D 17, 1788 (1978). For quark interchange models see, for instance, S. J. Brodsky and J. F. Gunion, *ibid.* 17, 848 (1978) and references therein. For quark-fragmentation models see, for instance. R. D. Field and R. P. Feynman, *ibid.* 15, 2590 (1977); Nucl. Phys. B136, 1 (1978); H. Fukuda and C. Iso, Prog. Theor. Phys. 57, 483 (1977); O. Sawada, *ibid.* 58, 1815 (1977); B. Anderson *et al.*, Phys. Lett. 69B, 221 (1977); Nucl. Phys. B135, 273 (1978); A. Capella *et al.*, Phys. Lett. 81B, 68 (1979); A. Capella *et al.*, LPTPE Report No. 79/23, 1979 (unpublished) and references therein.

[6]I. A. Schmidt and R. Blankenbecler, Phys. Rev. D 15, 3321 (1977); I. A. Schmidt, SLAC Report No. 203, 1977 (unpublished); R. Blankenbecler, SLAC Report No. PUB-2077, 1978 (unpublished).

[7]See, for instance, S. Nagamiya, in Proceedings of the 4th High Energy Heavy Ion Study, Berkeley, 1978 [LBL Report No. 7766 (unpublished)]; L. Schroeder *et al.*, Phys. Rev. Lett. 43, 1787 (1979).

[8]See, for instance, I. Otterlund *et al.*, University of Lund Report No. LUNDF6 (NFFK-7004), 1978 (unpublished) and references therein.

[9]H. D. Politzer, Phys. Rev. Lett. 30, 1346 (1973); D. J. Gross and F. Wilczek, *ibid.* 30, 1323 (1973).

[10]R. Blankenbecler and S. J. Brodsky, Phys. Rev. D 10, 2973 (1974); J. Gunion, *ibid.* 10, 242 (1974).

[11]A. M. Baldin, in *Proceedings of the 19th International Conference on High Energy Physics, Tokyo, 1978,* edited by S. Homma, M. Kawaguchi, and H. Miyazawa (Phys. Soc. of Japan, Tokyo, 1979), p. 455; Fiz. Elem. Chastits At. Yadra 8, 429 (1977) [Sov. J. Part. Nucl. 8, 429 (1977)] and references therein.

[12]G. Berlad *et al.*, Phys. Rev. D 13, 161 (1976), and references therein; Y. Afek *et al.*, in *Proceedings of the Topical Meeting on Multiparticle Production on Nuclei at Very High Energies, Trieste, 1976,* edited by G. Bellini, L. Bertocchi, and P. G. Rancoita (International Center for Theoretical Physics, Trieste, 1977), p. 591 and references therein.

[13]C. G. Callan and D. J. Gross, Phys. Rev. Lett. 22, 156 (1969).

[14]See, for instance, F. Dydak, lectures presented at the 17th Schladming Winter School, 1978 (unpublished) and references therein.

[15]M. May *et al.*, Phys. Rev. Lett. 35, 407 (1975); S. Stein *et al.*, Phys. Rev. D 12, 1884 (1975).

[16]J. H. Christenson *et al.*, Phys. Rev. Lett. 25, 1523 (1970); Phys. Rev. D 8, 2016 (1973).

[17]D. C. Hom *et al.*, Phys. Rev. Lett. 36, 1236 (1976).

[18]L. K. Klugberg *et al.*, Phys. Rev. D 11, 3105 (1975).

[19]S. D. Drell and T. M. Yan, Phys. Rev. Lett. 25, 316 (1970); Ann. Phys. (N.Y.) 66, 578 (1971).

[20]S. J. Brodsky and G. R. Farrar, Phys. Rev. Lett. 31, 1153 (1973); Phys. Rev. D 11, 1309 (1975).

[21]K. J. Anderson *et al.*, Phys. Rev. Lett. 42, 944 (1979).

[22](a) D. M. Kaplan *et al.*, Phys. Rev. Lett. 40, 435 (1978); (b) L. M. Lederman, in *Proceedings of the 19th International Conference on High Energy Physics, Tokyo, 1978,* edited by S. Homma, M. Kawaguchi, and H. Miyazawa (Phys. Soc. of Japan, Tokyo, 1979).

[23]R. Barate *et al.*, Phys. Rev. Lett. 43, 1541 (1979).

[24]S. Weinberg, Phys. Rev. Lett. 19, 1264 (1967); A. Salam, in *Elementary Particle Theory: Relativistic Groups and Analyticity (Nobel Symposium No. 8)* edited by N. Svartholm (Almqvist and Wiksell, Stockholm, 1968), p. 367.

[25]O. Chamberlain *et al.*, Phys. Rev. 100, 947 (1955).

[26]For an earlier version of the model see, e.g., Y. Afek *et al.*, Phys. Rev. D 20, 1160 (1979). In K. E. Lassila and J. D. Vary, Iowa State University Report No. IS-M-131, 1978 (unpublished). The W-production cross sections are greatly overestimated due to the use of "universality" and the disregard of the quark-model counting rules. See, G. Eilam and Y. Zarmi, Lett. al Nuovo Cimento 20, 479 (1977).

[27]J. W. Cronin *et al.*, Phys. Rev. D 11, 3105 (1975).

[28]F. Halzen and P. McIntyre, Phys. Rev. D 21, 726 (1980).

[29]L. S. Osborne *et al.*, Phys. Rev. Lett. 40, 1624 (1978).

[30](a) J. V. Allaby *et al.*, CERN Report No. 70-12, 1970 (unpublished); (b) T. Eichten *et al.*, Nucl. Phys. B44, 333 (1972); (c) M. Binkley *et al.*, Phys. Rev. Lett. 37, 571 (1976); (d) K. Heller *et al.*, Phys. Rev. D 16, 2737 (1977); (e) P. Skubic *et al.*, *ibid.* 18, 3115 (1978); (f) D. Chaney *et al.*, Phys. Rev. Lett. 40, 71 (1978).

[31]M. R. Walley *et al.*, University of Michigan Report No. HE 78-46, 1979 (unpublished).

[32]G. Berlad and A. Dar, Phys. Rev. D 21, 3133 (1980).

[33]V. V. Anisovich *et al.*, Nucl. Phys. B133, 477 (1978); N. N. Nikolaev and S. Pokorski, Phys. Lett. 80B, 290 (1979); N. N. Nikolaev and A. Ya. Ostapchuck, CERN Report No. TH 2575 (unpublished).

[34]A. Dar and F. Takagi, Phys. Rev. Lett. 44, 768 (1980); G. Berlad and A. Dar, Technion Report No. PH-79-69 (unpublished).

[35]A. Bialas and E. Bialas, Phys. Rev. D 20, 2854 (1979).

[36]E. M. Riordan *et al.*, Phys. Lett. 52B, 249 (1974); D. J. Fox *et al.*, Phys. Rev. Lett. 33, 1504 (1974); Y. Watanabe *et al.*, *ibid.* 35, 848 (1975); C. Chang *et al.*, *ibid.* 35, 901 (1975); H. L. Anderson *et al.*,

ibid. 37, 4 (1976); 38, 1450 (1977); A. Bodek *et al.*, Report No. SLAC-PUB-2248, 1979 (unpublished).
[37]E. M. Levin and L. L. Frankfurt, Pis'ma Zh. Eksp. Teor. Fiz. 2, 65 (1965) [JETP Lett. 2, 108 (1965)]; H. K. Lipkin and F. Sheck, Phys. Rev. Lett. 16, 71 (1966).
[38]A. Dar, K. J. Moriarty, and J. Trân Thanh Vân, in *High Energy Hadronic Interactions*, proceedings of the IX Rencontre de Moriond, Méribel-lès-Allues, France, 1974, edited by J. Trân Thanh Vân (CNRS, Paris, 1974), pp. 219–260.
[39]G. Nilsson, B. Anderson, and G. Gustafson, Phys. Lett. 83B, 379 (1979).
[40]J. Singh *et al.*, Nucl. Phys. B140, 189 (1978).
[41]S. P. Denisov *et al.*, Nucl. Phys. B61, 62 (1973); A. S. Carroll *et al.*, Phys. Lett. 80B, 319 (1979).
[42]G. Berlad, S. Dado, and A. Dar (unpublished).
[43]A. M. Baldin *et al.*, Yad. Fiz. 18, 79 (1973) [Sov. J. Nucl. Phys. 18, 41 (1974)]; A. M. Baldin *et al.*, Yad. Fiz. 20, 1201 (1974) [Sov. J. Nucl. Phys. 20, 629 (1975)]; Y. D. Bayukov *et al.*, Yad. Fiz. 19, 1266 (1974) [Sov. J. Nucl. Phys. 19, 648 (1974)].
[44]See, for instance, S. Frankel, Phys. Rev. Lett. 38, 1338 (1977), and references therein.
[45]See, for instance, A. M. Baldin, Ref. 11; A. M. Baldin *et al.*, in *Proceedings of the 7th International Conference on High Energy Physics and Nuclear Structure, Zurich*, 1977, edited by M. P. Locher (Birkhauser, Basel, 1977); JINR Report No. E1-11368, Dubna, 1978 (unpublished) and references therein.
[46]T. Hayashino *et al.*, Lett. Nuovo Cimento 16, 71 (1976); H. Fukushima *et al.*, *ibid.* 21, 1 (1978).
[47]Y. D. Bayukov *et al.*, Phys. Lett. 85B, 315 (1979).
[48]R. D. Amado and R. M. Woloshyn, Phys. Rev. Lett. 36, 1435 (1976).
[49]H. J. Weber and L. D. Miller, Phys. Rev. 16, 726 (1977).
[50]T. F. Fujita, Phys. Rev. Lett. 39, 174 (1977).
[51]V. V. Burov *et al.*, Phys. Lett. 67B, 46 (1977).
[52]L. L. Frankfurt and M. I. Strikman, Phys. Lett. 68B, 93 (1977).
[53]M. I. Gorenstein *et al.*, Yad. Fiz. 26, 788 (1977) [Sov. J. Nucl. Phys. 26, 414 (1977)].
[54]R. H. Landau and M. Gyulassy, Phys. Rev. C 19, 149 (1979).
[55]W. H. Sims *et al.*, Nucl. Phys. B41, 317 (1972).
[56]J. Hanlon *et al.* (Stony Brook–Carnegie Mellon–Fermilab–Technion Collaboration) (unpublished).